Global \ Local Geoid Models Accuracy Assessment in Palestine

Prepared by:

Mohammad Yaqoub Assfor **Mohannad Mohammad Turman**

Wafa Ali Zamareh

Supervisor:

Dr. Ghadi Younis - Zakarneh

Submitted to the College of Engineering

in partial fulfillment of the requirements for the degree of

Bachelor degree in Surveying Engineering

Palestine Polytechnic University

December 2019

Global \ Local Geoid Models Accuracy Assessment in Palestine

Prepared by:

Mohammad Yaqoub Assfor **Mohannad Mohammad Turman**

Wafa Ali Zamareh

Supervisor:

Dr. Ghadi Younis - Zakarneh

Signature of the project supervisor **Signature of the Head of the Department**

Name: …….. **Name: ……..**

Signature of the examining committee

……. **…….**

الإهداء

إلى الرحمة المهداة في زمن الظلم والظلمات ... رسول الله صلى الله عليه وسلم

إلى ورثة الأنبياء بعلمهم ...علماؤنا الأجلاء

إلى من عبدت لي بحبها طريق الجنان ... نبع الحنان أمي الحبيبة

إلى الذي تناثرت قطرات العرق على جبينه كقطر الندى مجتهدا ليوفر لي الحياة الكريمة ...والدي الحبيب

إلى الذين كانوا لي أنسا في معمعان الحياة ... إخواني وأخواتي

إلى الذين رفعوا لواء العشق الأبدي عبورا نحو جنان الرحمن شهداؤنا الأماجد

إلى البيارق الخفاقة في سماء العزة والإباء ... أسيراتنا وأسرانا البواسل

إلى أقصانا ومسرانا مَهْوَ القلوب وإلى كل ذرة من أرض الرباط فلسطين بأهلها وطهرها وقفارها..

إلى مسيرات العودة في شتى ربوع الوطن شمالها وجنوبها ...

إلى كل الإخوة والأخوات الذين ساهموا وعملوا في هذا المشروع، بتشجيعهم ودعائهم المتواصل، والذين كان لهم صدق مؤازرتنا في تنفيذه.

ثم إلى كل من علمني حرفاً أصبح سنا برقه يضيء الطريق أمامي إلى من علمني النجاح ... مشرفنا الدكتور غادي زكارنة

" وقل اعملوا فسيرى الله عملكم ورسوله والمؤمنون، وستردون إلى عالم الغيب والشهادة فينبئكم بما كنتم تعملون"

إليكم جميعا نهدي هذا العمل

ABSTRACT

Global \ Local Geoid Models Accuracy Assessment in Palestine

Prepared by:

Mohammad Yaqoub Assfor **Mohannad Mohammad Turman**

Wafa Ali Zamareh

Supervisor:

Dr. Ghadi Younis - Zakarneh

This project aims to apply field tests and accuracy assessment of the global geoid models and the locally used geoid models in Palestine, by means of statistical analysis using the network benchmarks in Palestine.

To evaluate the accuracy of the different geoid models, a group of precise leveling benchmarks was measured by classical GNSS methods (RTK). The ellipsoidal height (h) by GNSS and the orthometric height (H) by precise leveling provide a local geoid separation at the point (N). Geoid separation was calculated from the original global models and local models typically uploaded to the GNSS receivers. The differences were statistically analyzed to provide general descriptions. Also, local geoid fitting approaches were tested to enhance the accuracy of the global models.

Finally; description and accuracy analysis of the different geoid models were provided. The recommendation of the best field procedure that can be applied in the field was prepared, and the best result of accuracy came from (XGM2019e_2159) model.

الملخص

تقييم دقة انظمة الجيوئيد المحلية والعالمية في فلسطين

مجموعة العمل:

محمد يعقوب عصفور مهند محمد طرمان

وفاء علي زماعره

المشرف:

الدكتور غادي يونس زكارنه

يهدف هذا المشروع إلى تطبيق اختبارات ميدانية، وعمل تقييم لدقة نماذج الجيوئيد العالمية، والنماذج المستخدمة محلياً في فلسطين عن طريق رصد نقاط الارتفاع المرجعية الموجودة في فلسطين.

لتقييم دقة نماذج الجيوئيد المختلفة، تم في هذا المشروع رصد مجموعة من نقاط الارتفاع المرجعية باستخدام طرق الرصد المتعارف عليها و هي أنظمة الملاحة العالمية بالأقمار الصناعية(طريقة الرصد المتحرك)، وتم قياس الارتفاع عن سطح الإليبسويد(h) باستخدام أنظمة الملاحة العالمية بالأقمار الصناعية، وقياس الارتفاع الحقيقي عن سطح الجيوئيد (H) باستخدام التسوية الدقيقة وذلك بهدف معرفة ارتفاع الجيوئيد عن هذه النقطة، وتم حساب ارتفاع الجيوئيد عن طريق النماذج العالمية، والنماذج المحلية للجيوئيد التي يتم تحميلها الى مستقبلات أنظمة الملاحة العالمية بالأقمار الصناعية. الاختلافات بين أنظمة الجيوئيد العالمية وأنظمة الجيوئيد المحلية سوف تم تحليلها إحصائياً لإعطاء وصف عام عن هذا الاختلاف. وتم عمل اختبار دقة لملائمة نماذج الجيوئيد المحلية مع نماذج الجيوئيد العالمية.

وفي النهاية؛ تم إعطاء وصف عام وتحليل دقيق عن الاختلافات في نماذج الجيوئيد، وتم إعداد توصية لأفضل إجراء ميداني يمكن تطبيقه في هذا المجال للحصول على الدقة العالية، وأفضل نتيجة من الدقة تم الحصول عليها من نموذج الجيوئيد المسمى (XGM2019e_2159).

Acknowledge

We would like to express our endless gratitude for everyone who helped us during the graduation project, starting with the Palestine polytechnic university, college of engineering, civil and architectural engineering department for providing us with everything that we needed for the completion of the graduation project. Also, we would like to give our endless thanks for our supervisor Dr. Ghadi – Younis Zakarneh who didn't keep any effort in encouraging us to do a great job, providing our team with valuable information and advice to be better each time. Thanks for the continuous support and kind communication which great effect regarding feel interested in what we are working on.

Finally, we want to thank teachers for survey laboratories Eng. Ahmed Herbawi, and Groma Geosystems Company, especially Eng.Ihab Shaheen for supporting the field measurements, training, and data collection and transfer.

Table of Contents

الإهداء		**i**
Abstract		**ii**
الملخص		**iii**
Acknowledge		**iv**
Table of Contents		**v**
List of Figures		**vii**
List of Tables		**ix**
Chapter One: Introduction		**1**
1.1	Background	2
1.2	Problem Statement	2
1.3	Objective	2
1.4	Methodology	5
1.5	Project Scope	5
Chapter Two: Geodetic and Gravimetric Networks		**6**
2.1	Introduction	7
2.2	Horizontal Control Networks	7
2.2.1	Methods of Establishing a Horizontal Control Network	9
2.2.2	Reference Ellipsoids of the Horizontal Control Networks	11
2.2.3	Conversion Between Polar Coordinate and Cartesian Coordinate	16
2.3	Vertical Control Networks	18
2.4	The Three-Dimensional Networks	22
2.5	Gravimetric Networks	27
Chapter Three: Global and local gravity Geoid modeling		**30**
3.1	Introduction	31
3.2	The gravity field of the Earth	31
3.2.1	Laplace differential equation and Spherical Harmonics (SH)	33
3.2.2	The normalized SH	34
3.2.3	The normalized Legendre functions	35
3.2.4	Harmonic expansion of the Earth gravitational potential	36
3.2.5	Derivatives of the potential of the Earth	38
3.2.6	The spherical harmonic expansion of the Earth’s gravity field	42
3.3	The local potential modeling	44
3.3.1	Stokes formula and remove-restore method	44
3.3.2	GNSS/Leveling	45
3.3.3	Digital finite elements height reference surface (DFHRS)	45
3.3.3.1	Principles of DFHRS	46
3.3.3.2	Extension of DFHRS to physical observations	49
3.3.4	Least Squares Collocation	51
3.4	Integrated Geodesy	53
3.5	State of the art in the gravity field modeling	54
Chapter Four: Data and Analysis		**57**
4.1	Introduction	58
4.2	Global Evaluation of the Geoid Models.	60
4.3	Local Evaluation of the Geoid Models	61
4.3.1	Local Evaluation Steps	61
4.3.2	EGM96 Evaluation	62

4.3.3 EGM2008 Evaluation 63
4.3.4 EIGIN-5C Evaluation 65
4.3.5 EIGIN-6C4 Evaluation 66
4.3.6 XGM2019_2159 Evaluation 68
Chapter Five: Conclusions and Recommendations **71**
5.1 Conclusions 72
5.2 Recommendations 73
Reference **74**
List of Acronyms **75**
List of Symbols **76**

List of Figures

Nr.	Description	Page
1.1	Geoid of the earth	2
1.2	Geoid Height& Ellipsoidal Height& Orthometric Height	4
2.1	Triangulation & Trilateration & Traverse	8
2.2	Triangulation with baseline extension net and Laplace azimuth (principle)	9
2.3	Trilateration with Laplace azimuth (principle)	9
2.4	Traverse connecting two control points (principle)	10
2.5	Locally best fitting “conventional” ellipsoid	13
2.6	Regionally best fitting ellipsoid	13
2.7	Mean Earth ellipsoid	14
2.8	Horizontal control network of the U.S.A. (NAD83), with first- and second-order, triangulation, and traverses	15
2.9	Primary triangulation net of Germany (DHDN90).	15
2.10	Spherical Coordinates	16
2.11	Leveling network (principle).	18
2.12	North American Vertical Datum of 1988 leveling network	20
2.13	United European Leveling Net (2008)	20
2.14	Primary leveling network of Germany	21
2.15	GNSS network constructed from individual blocks (principle)	24
2.16	GNSS network constructed from baselines to permanent GNSS stations	25
2.17	Absolute gravimeters	28
2.18	Relative gravimeter	28
2.19	Primary gravity net (red circles) of Germany	29
3.1	Geographic coordinates (λ, ϕ, h) and the spherical coordinates (r, λ, $\overline{\phi}$)	33
3.2	The gravitational and centrifugal accelerations of the Earth	39
3.3	Height anomaly ζ vs. geoid height N	41
3.4	The relation between orthometric height H, ellipsoidal heights h and geoid undulation N	46
3.5	DFHRS patches and meshes, where thick lines represent the patch boundary and thin lines represent the meshes	48
3.6	The principle of harmonic coefficients calculation in EIGEN06c model	54

4.1	ICGEM Site	60
4.2	The distribution of the group of precise leveling benchmarks in Palestine.	62
4.3	Palestine Geoid Model (EGM96)	62
4.4	Palestine Geoid Model (EGM2008)	64
4.5	Palestine Geoid Model (EIGIN-5C)	65
4.6	Palestine Geoid Model (EIGEN-6C4)	67
4.5	Palestine Geoid Model (XGM2019e_2159)	69

List of Tables

Nr.	Description	Page
2.1	Parameters of reference ellipsoids (rounded values)	12
2.2	Reference ellipsoids and origin points of some geodetic datums	14
3.1	Some of the common global gravity models with their data sources	42
3.2	The potential related observations and their linear operators L(T)	52
3.3	Examples of satellite only and combined global geoid models	55
4.1	Global Evaluation of the Geoid Models.	61
4.2	Ellipsoidal height (h), Orthometric height (H) and Geoid height (N) of the group of precise leveling benchmarks in Palestine.	61
4.3	Result of the Geoid Height from (EGM96)	63
4.4	Result of the Geoid Height from (EGM2008)	64
4.5	Result of the Geoid Height from (EIGEN-5C)	66
4.6	Result of the Geoid Height from (EIGEN-6C4)	68
4.7	Result of the Geoid Height from (XGM2019e_2159)	69
5.1	The accuracy of the models	72

Chapter One:

Introduction

1.1 Background

1.2 Problem Statement

1.3 Objective

1.4 Methodology

1.5 Project Scope

Introduction

1.1 Background

Geodesy is a branch of applied mathematics which determines by observation and measurement the exact positions of points and areas of large portions of the earth's surface, the shape and size of the earth, and the variations of terrestrial gravity. The points positions are measured and identified by two components (Positions), Horizontal Positions and Vertical Positions. [1]

Horizontal Positions are the location of a point relative to two axes, the equator and the prime meridian on the globe, or x and y axes in a plane coordinate system, and the point position is defined in polar coordinates (λ, ϕ) or by Cartesian coordinates (geocentric coordinates) (X, Y), it can possible to convert between these coordinate systems by a set of equations and parameters, and also convert from these coordinate systems to Easting and Northing projected coordinates by using map projections. [7]

Vertical Positions are the height of a point relative to some reference surface, such as mean sea level, a geoid, or an ellipsoid, and there are several different ways to measure heights. [7]

The geoid is a level, or equipotential surface, where the gravity potential is a constant value. The gravity force vector acts perpendicular to this surface. A good example of a level surface would be a large body of water where the force of gravity acts on the water such that a constant surface is formed, see figure (1.1). [1]

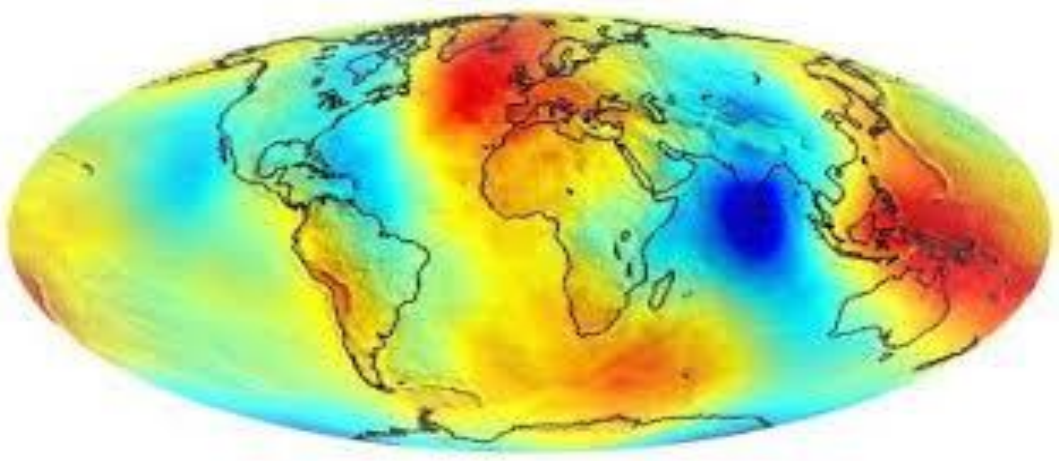

Figure (1.1): Geoid of the earth

The **orthometric (geoid) height** of a point of the Earth Surface is the distance (H) from the point to the geoid, and we can measure it by precise leveling. [7]

The Global Navigation Satellite Systems (GNSS) are systems of satellites that continuously provide positioning possibilities with global coverage. They allow small electronic receivers to determine their location (longitude, latitude, and altitude) to high precision (within a few meters to sub-centimeter) using time radio signals transmitted along a line of sight by satellites. The signals also allow the electronic receivers to calculate the current local time to high precision. [2]

The global geocentric reference frame and coordinates system is known as the World Geodetic System 1984 (WGS84) has been developed continuously since its creation in the mid-1980s. The WGS84 continues to provide a single, common, accessible 3-dimensional coordinate system for global data collected from different sources. Some of these geospatial data require a high degree of accuracy and require a global reference frame that is free of any significant distortions or biases. For this reason, a series of improvements to WGS84 were developed in the past years, which served to refine the original version. The data collected by the GNSS according to the WGS84 reference system can easily be transformed into any local coordinates system. [2]

Real-Time Kinematic (RTK) is one of the most common poisoning methods in GNSS. It is a Kinematic method of the GNSS survey carried out in real-time. The Reference Station has a radio (link/ internet connection) attached and rebroadcasts the data and correction it receives from the satellites to the rover station. The virtual reference station (VRS) concept of RTK can help to satisfy this requirement using a network of reference stations, to cover a wide area and high positioning accuracy using continuously operation network of reference stations and internet connections to the users. [2]

The **ellipsoidal height** of a point of the Earth Surface is the distance (h) from the point to the ellipsoid, and we can measure it by GNSS. [7]

The **geoid height above the ellipsoid (N)** is the difference between the ellipsoidal height and orthometric (geoid) height. [7]

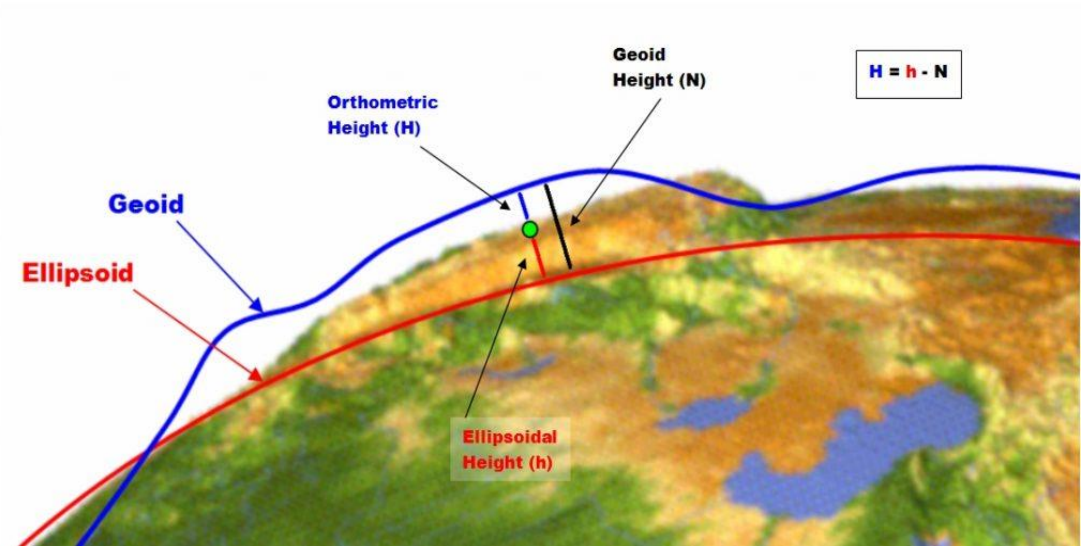

Figure (1.2): Geoid Height& Ellipsoidal Height& Orthometric Height

1.2 Problem Statement

The global navigation system gives (1) centimeter accuracy of measurement in both horizontal and vertical coordinates in Geodetic systems like; WGS84, but The global navigation system does not reach (1) centimeter accuracy in local vertical measure much worse accuracy up to many centimeters; due to the difference in geoid systems, and satellite geometry, these errors make it impossible to make precise leveling using GNSS, therefore users are forced to use additional instrument (like level) and more working staffs, so to solve the problem, it is important to use a proper precise geoid model to define heights by GNSS in Palestine, here; an evaluation of the common models is applied to help to decide the most proper one.

1.3 Objective

These project aims are:

- Apply field tests and accuracy assessment of the global geoid models and the locally used geoid models in Palestine, by means of statistical analysis using the network benchmarks in Palestine.
- Provide description and accuracy analysis of the different geoid models.
- Prepared recommendation of best field procedure that can be applied in the field.
- Know the appropriate geoid system in Palestine to obtain the required accuracy.

1.4 Methodology

The Methodology of work in this project will be achieved by observing a group of benchmarks using the RTK (Real-Time Kinematic) GNSS (The Global Navigation Satellite Systems**)** surveying for fixed period time (2 minutes), and by precise leveling, then evaluating the accuracy of the different geoid models, and find the appropriate geoid system in Palestine. Finally, the different geoid models will compare to decide the best fitting geoid for Palestine.

1.5 Project Scope

This project consists of the following chapters:

The first chapter is "Introduction", it describes an introduction about geodesy, and GNSS, the problem statement of the project, the objective of the project, the methodology of the project, and project scope.

The second chapter is "Geodetic and Gravimetric Networks", this chapter mainly discusses geodetic networks, types of geodetic networks (vertical, horizontal, and three dimensional) and gravimetric networks, the methods and the principles.

The third chapter is "Global and local gravity field modeling", it describes the general methods for global and local potential modeling using Spherical Harmonics, the Stokes formula, least-squares collocation, and the Finite elements methods are introduced. The principle of Integrated Geodesy is also introduced, and a general overview of the state-of-the-art of the latest global and local gravity and geoid models is provided.

The fourth chapter is "Data and Analysis", it describes the Global and Local evaluation of the Geoid models, and it explains and shows the main result of this project.

The fifth chapter is "Conclusion and Recommendation", it provides the description and accuracy analysis of the different geoid models, and it prepares the recommendation of the best field procedure that can be applied in the field.

Chapter Two:

Geodetic and Gravimetric Networks

2.1 Introduction

2.2 Horizontal Control Networks

2.3 Vertical Control Networks

2.4 The Three-Dimensional Networks

2.5 Gravimetric Networks

Geodetic and Gravimetric Networks

2.1 Introduction

Geodetic and gravimetric networks consist of monumented control points that provide the reference frames for positioning and gravity-field determination. In the sequel, we concentrate on regional networks that are established nation- or continent-wide. They serve as the basis for all kinds of surveying and navigation, as well as for geoinformation systems including topographic and thematic map series, and for the investigation of recent geodynamics. Regional networks are increasingly derived from or integrated into global reference frames established and maintained by international conventions. Local networks are established, e.g., for engineering and exploration projects, real estate surveys and crustal movement investigations. They generally follow similar rules as regional networks at design, measurement, and evaluation adapted to the specific demands and peculiarities of the respective problem. [3]

Until recently, horizontal and vertical control networks have been established separately, following the classical treatment of (horizontal) positioning and heightening. These networks still are the basis of national geodetic reference systems, and they even have been partly combined with continent-wide systems. For some decades, geodetic space methods allow the establishment of three-dimensional (3D) networks orientated with respect to a geocentric reference system. Today, these methods are characterized by very efficient procedures and homogeneous results of high accuracy, and consequently, they are superseding the classical control networks. Strong endeavors are made now to integrate these networks into the 3D frame which also requires the inclusion of a geoid model. Gravity networks serve the different needs of geodesy and geophysics, with the reference provided either by a global gravity standardization net or by absolute gravimetry; they are now also tied to the 3D geodetic reference frame. [3]

This chapter mainly discusses Geodetic and Gravimetric Networks, the methods, principles.

2.2 Horizontal Control Networks

National horizontal control networks were established from the eighteenth century until the 1980s, where the networks' design, observation, and computation methods changed with the available techniques. Computations were carried out on a conventional reference ellipsoid fitted to the survey area. Since the 1960s, spatial geodetic methods have allowed orientation

of the classical networks with respect to the global geocentric reference system and control of scale and systematic distortions. In the following, we describe the design of these networks, the measurement and computation techniques applied, the accuracy achieved, and the orientation with respect to the Earth's body (geodetic datum). Having served (and serving) as a basis for many applications in surveying and mapping, they are still of relevance and now in a state of transition to the global 3D reference frame. [3]

Horizontal control networks have been realized by trigonometric (triangulation) points, which in principle should be distributed evenly over the country. One distinguishes between different orders of trigonometric points, from first-order or primary (station separation 30 to 60 km) to second-order (about 10 km) to fourth- or even fifth-order (down to 1 to 2 km) stations, where the state of the networks' coverage strongly depends on the development of the respective region or country. The maximum distance between first-order points was determined by terrestrial measurement methods, which required intervisibility between the network stations. Consequently, first- and partly also second-order stations were established on the top of hills and mountains; observation towers (wooden or steel constructions with heights of 30 m and more) were erected especially in flat areas. The stations have been permanently marked by underground and surface monuments (stone plates, stone or concrete pillars, bolts in hard bedrock). Eccentric marks have been set up in order to aid in the recovery and verification of the center mark. [3]

Classical horizontal control networks have been observed by the methods of triangulation, trilateration, and traversing, see figure (2.1).

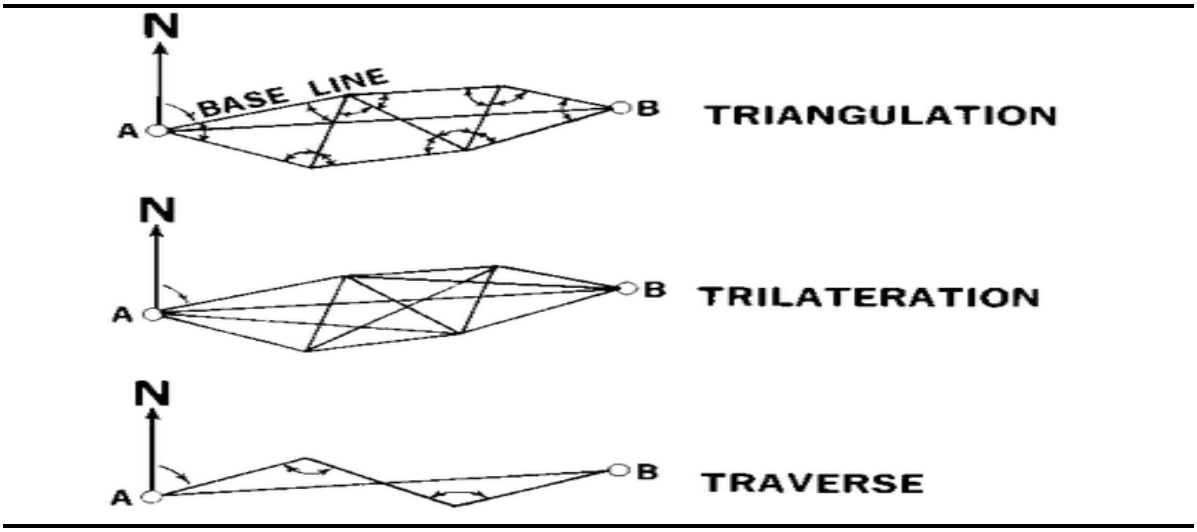

Figure (2.1): Triangulation & Trilateration & Traverse

2.2.1 Methods of Establishing a Horizontal Control Network

Triangulation, all angles of the triangles formed by the trigonometric points are observed with a theodolite figure (2.2). The instrument is set up on the observation pillar or tower; at large distances, the targets are made visible by light signals. Either direction (successive observation of all target points) or angles (the separate measurement of the two directions comprising one angle) are observed in several sets (i.e., in both positions of the telescope), distributed over the horizontal circle of the theodolite. The scale of a triangulation network is obtained from the length of at least one triangulation side, either derived from a short baseline through a baseline extension net or measured directly by a distance meter. Astronomic observations provide the orientation of the network, where an astronomic azimuth (Laplace azimuth) is needed for the horizontal orientation. [5]

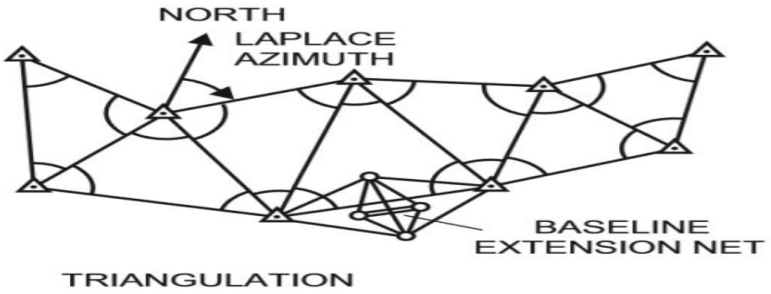

Figure (2.2): Triangulation with baseline extension net and Laplace azimuth (principle). [5]

Trilateration employs electromagnetic distance meters in order to measure the lengths of all triangle sides of a network, including diagonals figure (2.3). Again, at least one Laplace azimuth is needed for the orientation of the net. Electromagnetic distance measurements put fewer demands on the stability of observation towers as compared to angular measurements, and the use of microwaves makes the method more independent from weather conditions. [5]

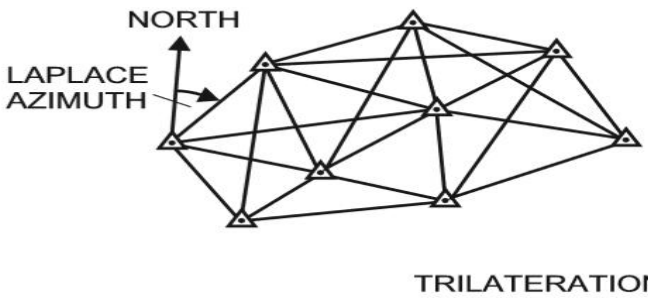

Figure (2.3): Trilateration with Laplace azimuth (principle). [5]

Traverses combine distance and angular measurements, where the traverse stations are arranged along a profile between already existing control points. The traverse stations may be either transformed into the national reference system by means of the control points or immediately calculated in that system if astronomic (Laplace azimuth) or terrestrial orientation is available, figure (2.4) gives some examples. Traversing represents a very effective and flexible method for establishing horizontal control, with no more need to establish stations on hilltops. It has been employed primarily for the densification of higher-order networks. [3]

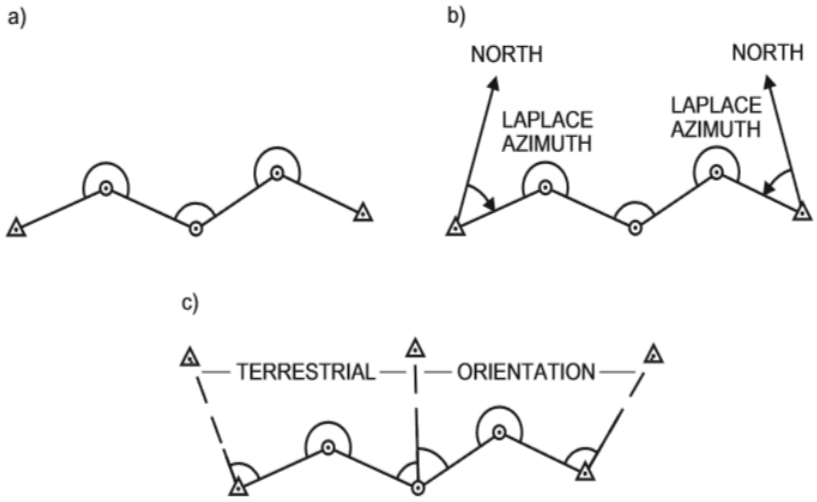

Figure (2.4): Traverse connecting two control points (principle): a) without additional orientation, b) with an orientation by Laplace azimuths, c) with an orientation by directions to control points. [3]

Horizontal control networks have also be formed by combining the methods of triangulation, trilateration, and traversing. Such networks are very stable in design, and allow the establishment of first- and second-order control simultaneously. Optimization methods have been developed for the design and survey of trigonometric networks. Starting from the demands on accuracy and reliability, these methods provide information on the optimum point configuration and the distribution of the measurements in the network given the limitations of available equipment and the maximum allowable cost of the survey. [3]

2.2.2 Reference Ellipsoids of the Horizontal Control Networks

First- and some second-order horizontal control networks have been calculated on a reference ellipsoid within the system of ellipsoidal coordinates. Lower-order networks are primarily calculated in planar Cartesian coordinates, after conformal mapping of the ellipsoid

onto the plane. The network calculation started with the reduction of the observed horizontal angles/directions and spatial distances to the ellipsoid, where the gravity-field-related reductions (deflections of the vertical, geoid height) were not considered during earlier surveys. The adjustment was carried out either by the method of conditions or by variation of the coordinates, with redundancy resulting from triangle misclosures, diagonals in trilateration quadrilaterals, and additional baselines and Laplace azimuths. The coordinates' transfer from an initial point (see below) was based on the solutions of the direct resp. inverse problem on the ellipsoid. Among the deficiencies of this classical "development method" are the neglecting of the deflections of the vertical, the inadequate reduction of distances on the ellipsoid, and especially the step by step calculation of larger networks, with junction constraints when connecting a new network section to an existing one. This led to long-wavelength network distortions of a different type, with regionally varying errors in scale ($1\ 0^{-5}$ and more) and orientation. Coordinate errors with respect to the initial point increased from a few decimeters over about 100 km to about 1 m over several 100 km and reached 10 m and more at the edges of extended continent-wide networks. [3]

The geodetic datum of a horizontal control network comprises the parameters of the reference ellipsoid and of the network's orientation with respect to the Earth's body. Conventional ellipsoids, as computed by the adjustment of several arc measurements, were introduced during earlier geodetic surveys. Some horizontal networks refer to locally best-fitting ellipsoids, as derived from a minimum condition on the observed vertical deflections.

$$\sum (\xi 2 + \eta 2) \ = \ min \tag{2-1}$$

The orientation of the ellipsoid was realized by defining the ellipsoidal coordinates of a fundamental (initial) point, also called network origin, and by conditions for the parallelism of the axes of the ellipsoidal and the global geocentric system.

In earlier surveys, the coordinates of the fundamental point were fixed by postulating equality between observed astronomic latitude, longitude, and orthometric height and the corresponding ellipsoidal quantities. This is identical to setting the deflection of the vertical and the geoid height of the fundamental point to zero:

$$\xi f \ = \ 0, \ \eta f \ = \ 0, \ Nf \ = \ 0 \tag{2-2}$$

Table (2.1) gives the parameters of some reference ellipsoids that have been used for national geodetic surveys:

Table (2.1): Parameters of reference ellipsoids (rounded values) [4]

Name, Year	**Semi-major axis *a* (m)**	**Reciprocal flattening 1/*f***
Airy, 1830	6 377 563.3964	299.32496459
Bessel, 1841	6 377 397.155	299.15281285
Clarke, 1866	6 378 206.4	294.9786982
Clarke, 1880 Palestine	6 378 300.79	293.466307656
Everest 1830	6 377 276.3458	300.80117
Fischer 1960 Modified	6 378 155	298.3
GRS80	6 378 137	298.257221008827
Helmert 1906	6 378 200	298.3
Krassovsky 1940	6 378 245	298.3
WGS84	6 378 137	298.257223563

This strategy provides a good approximation of the ellipsoid to the geoid close to the origin but may lead to larger deviations at more remote areas figure (2.5). If a sufficient number of vertical deflection points were available and well distributed over the area of calculation, the minimum condition was used. It permits the determination of the deflection of the vertical in the fundamental point and at extended networks also the parameters of a best-fitting ellipsoid. This procedure led to an optimum fitting over the whole area and kept the deflections of the vertical small. In many cases, the geoid height of the origin point was defined indirectly by reducing the baselines onto the geoid and treating them as ellipsoidal quantities figure (2.6). The minimum condition for the geoid heights was seldom applied using relative geoid heights calculated from astronomic leveling. [3]

$$\sum N2 = min \tag{2-3}$$

The parallelism of the axes of the ellipsoidal and the geocentric system was achieved by the Laplace equation. In extended networks, several baselines and Laplace stations often were established at distances of a few 100 km in order to control the error propagation through the network with respect to scale and orientation (effects of lateral refraction). More recently, the ellipsoid parameters of a geodetic reference system have been introduced, and the ellipsoid has been optimally fitted to the geoid, figure (2.8). Table (2.2) lists the ellipsoids and the origin points used for some geodetic datums. [3]

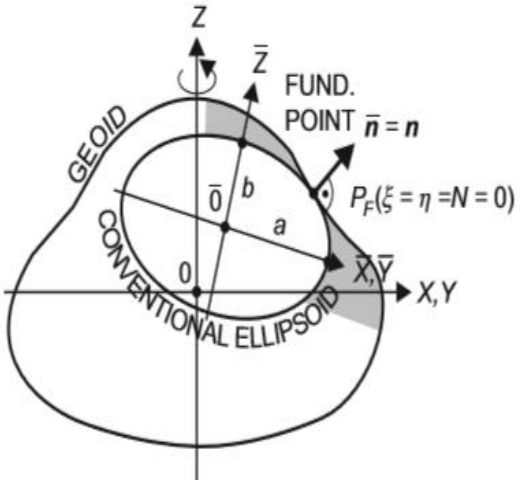

Figure (2.5): Locally best fitting "conventional" ellipsoid. [3]

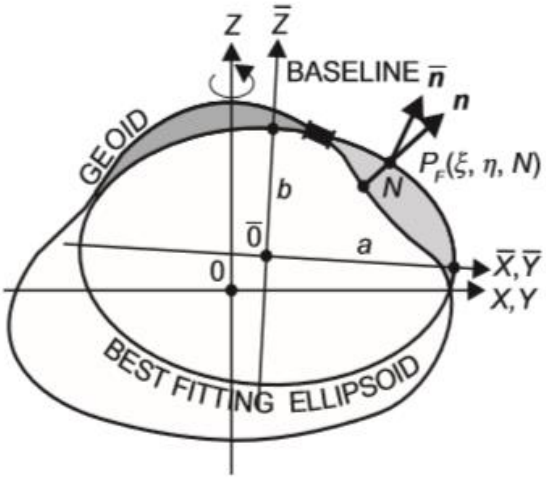

Figure (2.6): Regionally best fitting ellipsoid. [3]

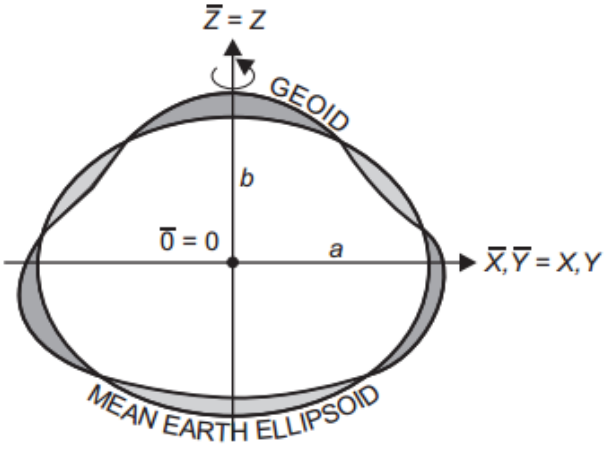

Figure (2.7): Mean Earth ellipsoid. [3]

Table (2.2): Reference ellipsoids and origin points of some geodetic datums [3]

Geodetic datum	Reference ellipsoid	Name of origin	Origin	
			Latitude	Longitude
Australian Geodetic 1984 (AGD84)	GRS67	Johnston	−25°57’	133°13’
Deutsches Hauptdreiecksnetz (DHDN), Germany	Bessel 1841	Rauenberg/Berlin	52°27’	13°22’
European Datum 1950 (ED50)	Intern.Ellipsoid 1924	Potsdam, Helmertturm	52°23’	13°04’
Indian	Everest 1830	Kalianpur	24°07’	77°39’
North American 1927 (NAD27)	Clarke 1866	Meades Ranch, Kansas	39°13’	261°27’
North American 1983 (NAD83)	GRS80	Geocentric		
Ordnance Survey of Great Britain 1936 (OSG36)	Airy 1830	Herstmonceux	50°52’	0°21’
Pulkovo 1942, former Soviet Union	Krassovski 1940	Pulkovo	59°46’	30°20’
South American 1969 (SAD69)	GRS67	Chua, Brazil	−19°46’	311°54’

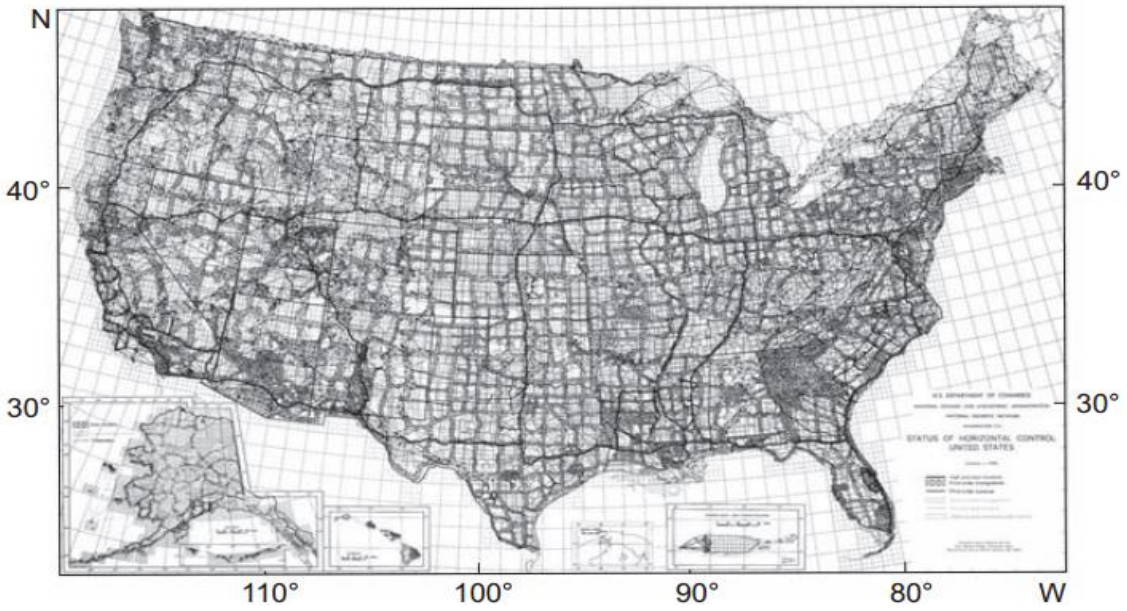

Figure (2.8): Horizontal control network of the U.S.A. (NAD83), with first- and second-order, triangulation, and traverses. [5]

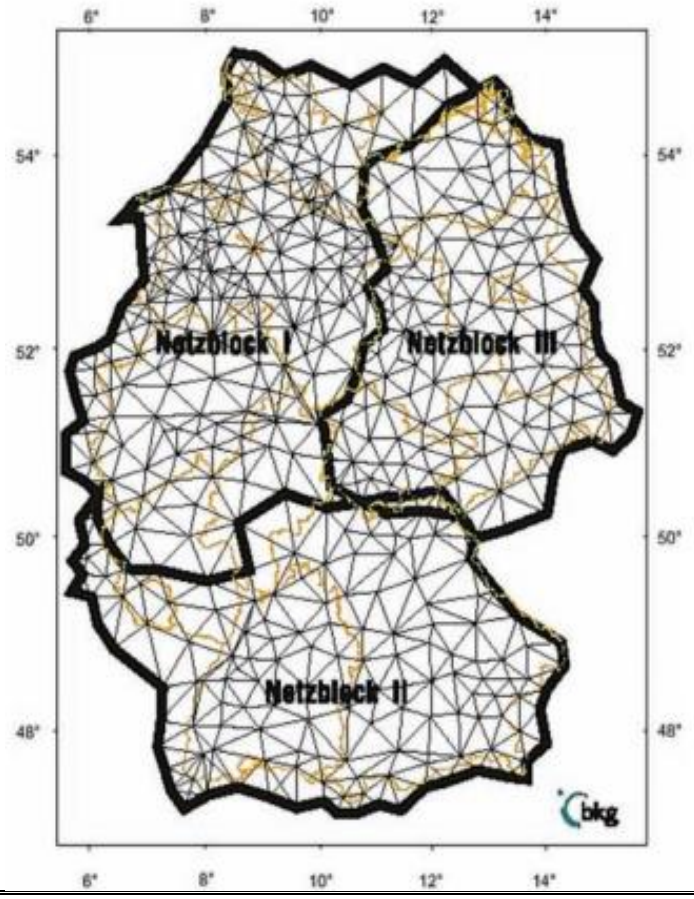

Figure (2.9): Primary triangulation net of Germany (DHDN90). [5]

2.2.3 Conversion Between Polar Coordinate and Cartesian Coordinate

- **Spherical Coordinates**

Considering the earth as a sphere with radius R, the point position is defined in polar coordinates (λ, ϕ, h) or by cartesian coordinate (geocentric coordinate) (X, Y, Z). An approximate radius of the earth R≈6371 km. [4]

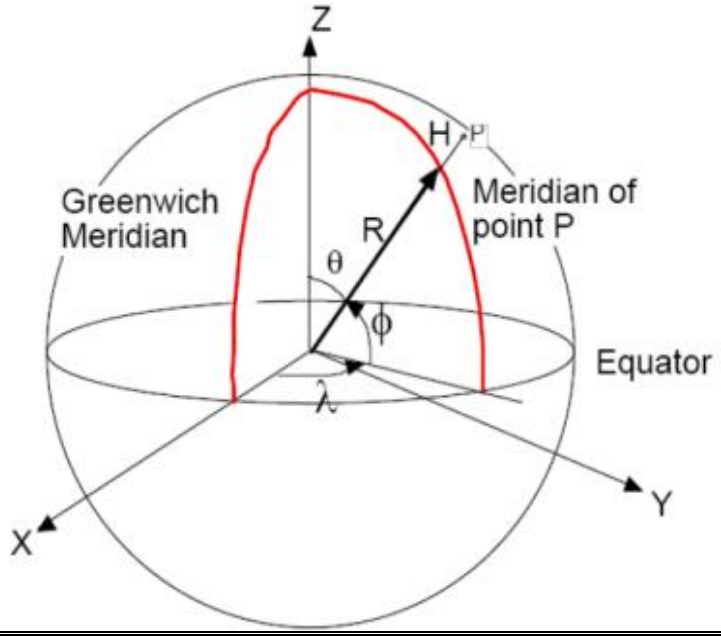

Figure (2.10): Spherical Coordinates. [4]

The conversion from polar coordinate to cartesian coordinate can be calculated as follows:

$$X = (N + h)\cos\phi\cos\lambda \quad (2\text{-}4)$$

$$Y = (N + h)\cos\phi\sin\lambda \quad (2\text{-}5)$$

$$Z = ((1 - e^2)N + h)\sin\phi \quad (2\text{-}6)$$

Where:

$$e^2 = \frac{a^2 - b^2}{a^2} = f(2 - f) \quad (2\text{-}7)$$

$$b = a(1 - f) \quad (2\text{-}8)$$

$$N = \frac{a}{\sqrt{1 - e^2\sin^2\phi}} \quad (2\text{-}9)$$

The conversion from cartesian coordinate to polar coordinate can be calculated as follows:

- **Iterative solution (Torge Method)**

$$\lambda = \tan^{-1}\frac{Y}{X} \qquad \text{(Does not need iteration)} \tag{2-10}$$

$$h = \frac{\sqrt{X^2+Y^2}}{\cos\phi} - N \tag{2-11}$$

$$\phi = \tan^{-1}\left(\frac{Z}{\sqrt{X^2+Y^2}}\left(1 - e^2\frac{N}{N+h}\right)^{-1}\right) \tag{2-12}$$

The initial value to start the iterative solution:

$$\phi = \tan^{-1}\frac{Z}{\sqrt{X^2+Y^2}}(1-e^2)^{-1} \tag{2-13}$$

- **Non-Iterative solution (Bowring Method)**

$$\lambda = \tan^{-1}\frac{Y}{X} \tag{2-14}$$

$$\phi = \tan^{-1}\left[\frac{Z+e'^2 b\sin^3 u}{P-e^2 a\cos^3 u}\right] \tag{2-15}$$

$$h = P\cos\phi + Z\sin\phi - a\sqrt{1-e^2\sin^2\phi} \tag{2-16}$$

Where:

$$u = \tan^{-1}\left[\frac{aZ}{bP}\right] \tag{2-17}$$

$$P = \sqrt{X^2+Y^2} \tag{2-18}$$

$$e'^2 = \frac{a^2-b^2}{b^2} = \frac{e^2}{(1-f)^2} \tag{2-19}$$

$$f = \frac{a-b}{a} = 1-(1-e^2)^{1/2} \tag{2-20}$$

2.3 Vertical Control Networks

Traditionally, national vertical control networks have been established separately from horizontal control nets. This is due to the demand that heights have to be defined with respect to the gravity field and a corresponding reference surface (e.g., geoid, quasigeoid) rather than to the ellipsoidal system used for horizontal positioning.

Vertical control networks are surveyed by geometric (also spirit or differential) leveling and occasionally also by hydrostatic leveling, the control points being designated as benchmarks. According to the leveling procedure and the accuracy achieved, national geodetic surveys distinguish between different orders of leveling. First-order leveling is carried out in closed loops (loop circumferences of some 100 km) following the rules for precise leveling. An accuracy of 0.5 ... 1 $mm\sqrt{s}\,(km)$ is achieved at double-run leveling (s is the length of the leveled line), but systematic effects may lead to error accumulation over long distances. The loops are composed of leveling lines connecting the nodal points of the network figure (2.7). The lines, in turn, are formed by leveling runs that connect neighboring benchmarks (average spacing 0.5 to 2 km and more). The first-order leveling network generally is densified by second to fourth-order leveling, with diminishing demands on accuracy. [5]

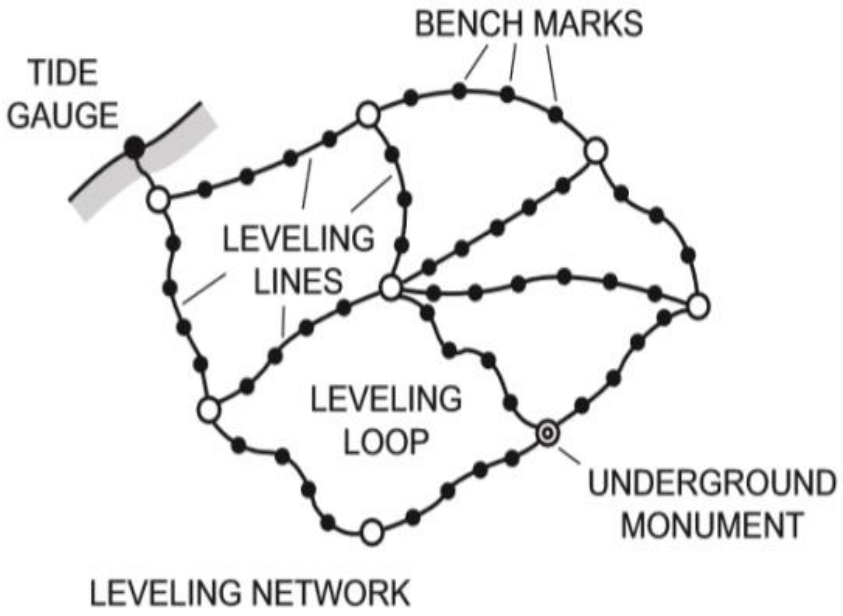

Figure (2.11): Leveling network (principle). [5]

Leveling lines generally follow main roads, railway lines, and waterways. The benchmarks consist of bolts in buildings, bedrock, or on concrete posts. Long pipes have been set up in alluvial regions. Underground monuments are established in geologically stable areas in order to control the network stability with respect to variations with time. First-order networks should be reobserved at time intervals of some 10 years, as regional and local height changes can reach one mm/year and more, especially in areas that experience vertical crustal movements of tectonic, isostatic or man-made origin. [5]

Prior to the adjustment of a leveling network, the observed raw height differences have to be transformed either to geopotential differences or to differences of normal or orthometric heights by taking surface gravity into account. The adjustment then utilizes the loop misclosure condition of zero and is carried out either by the method of condition equations or, preferably, by the method of parameter variation. [5]

The vertical datum of a national height system generally is defined by mean sea level (MSL) as derived from tide gauge records. The zero height surface running through the defining MSL depends on the choice of the height system and is either a level surface close to the geoid (orthometric heights) or the quasigeoid (normal heights). In future, high-resolution geoid or quasigeoid models may also serve for the definition of the vertical datum, again being realized through the heights of fundamental benchmarks. If based on MSL from different tide gauges, national height systems may differ by some dm to one m and more, between each other and from the geoid as a global reference surface. This is due to the effect of sea surface topography, which additionally causes network distortions if the vertical datum is constrained to MSL of more than one tide gauge. [5]

Mean sea level (MSL) (often shortened to sea level) is an average level of the surface of one or more of Earth's oceans from which heights such as elevation may be measured. MSL is a type of vertical datum – a standardized geodetic datum – that is used, for example, as a chart datum in cartography and marine navigation, or, in aviation, as the standard sea level at which atmospheric pressure is measured to calibrate altitude and, consequently, aircraft flight levels. A common and relatively straightforward mean sea-level standard is the midpoint between a mean low and mean high tide at a particular location. [5]

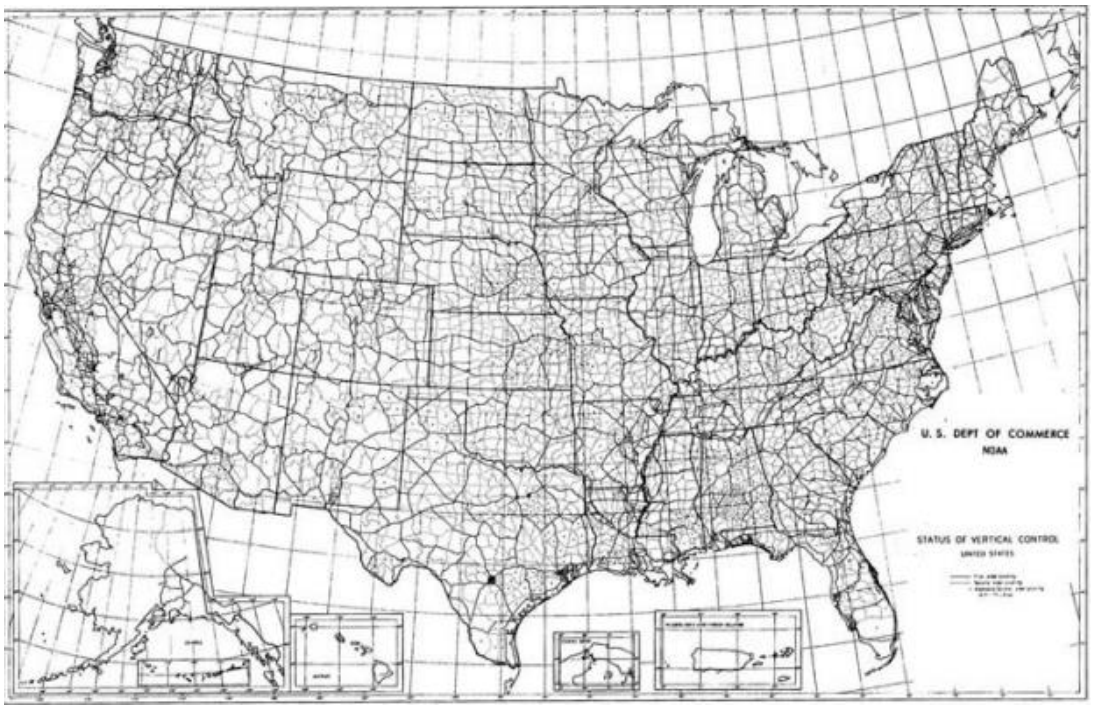

Figure (2.12): North American Vertical Datum of 1988 leveling network [3]

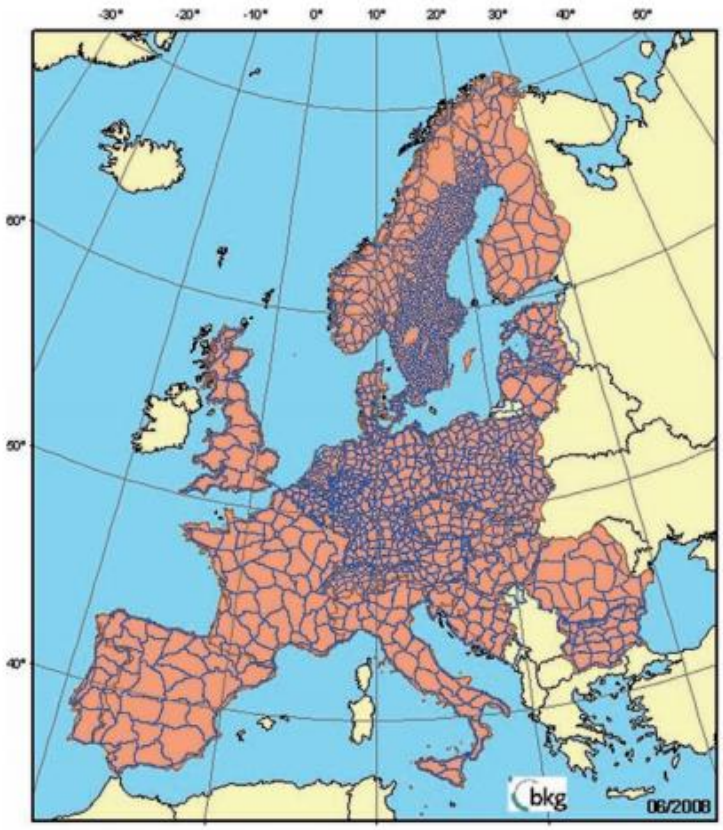

Figure (2.13): United European Leveling Net (2008) [3]

Leveling networks are characterized by high accuracy, but systematic errors may accumulate over large distances. A severe handicap of classical leveling networks is the significant loss of benchmarks with time due to human activities, and the manifold height changes occurring at local and regional scales. Due to the timeconsuming measurement procedure, repetition or restoration surveys are feasible only after longer time intervals, which leads to a rapid network decay. A more rapid establishment of vertical control networks has been achieved occasionally by trigonometric leveling, and a drastic change is now taking place by GNSS heightening in connection with high-resolution geoid or quasigeoid models, In this way, vertical control networks are integrated into and gradually substituted by 3D reference systems. The time-consuming spirit leveling required for the establishment and maintenance of the classical vertical control networks may become mostly superfluous. On the other hand, geometric leveling will maintain its importance over shorter distances, and especially in areas of recent crustal movements, such as regions of land subsidence and zones of Earthquake or volcanic activity. [3]

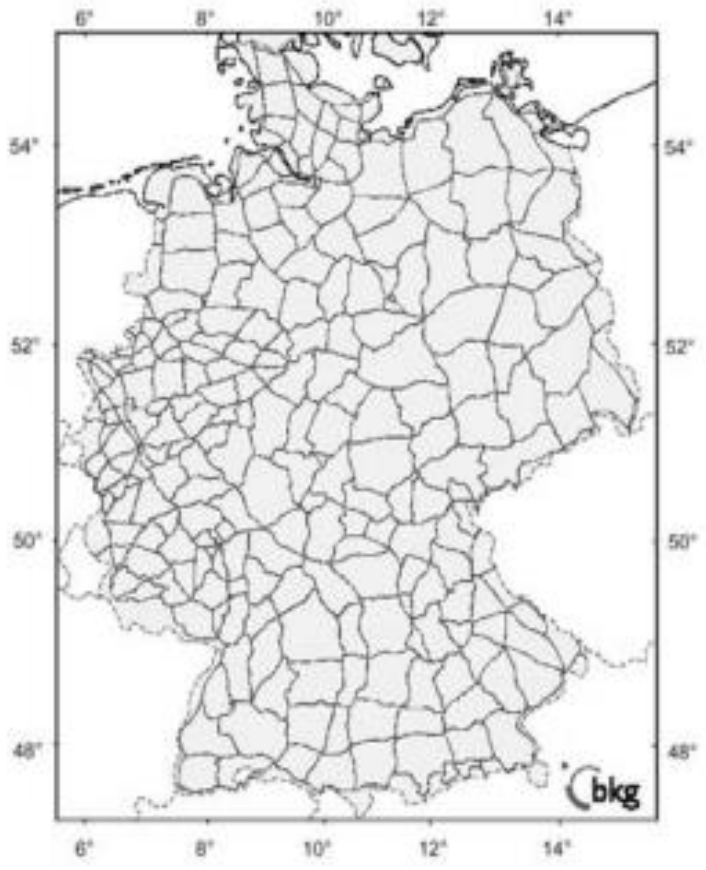

Figure (2.14): Primary leveling network of Germany [3]

2.4 The Three-Dimensional Networks

Starting at the end of the 1980s, GNSS techniques have more and more entered into geodesy and are now primarily used at all scales for positioning and navigation. This has led to a drastic change at the establishment and maintenance of geodetic control networks which are now definitely 3D and based on satellites as system carriers. [3]

Nowadays, the global geodetic reference is well established and provided by the International Terrestrial Reference Frame (ITRF) being the realization of the International Terrestrial Reference System. The ITRF stations are given with their 3D geocentric coordinates (cm-accuracy) for a certain reference epoch, and with corresponding horizontal velocities. The International GNSS Service (IGS) provides a powerful contribution to the ITRF and serves for densifying this global reference frame. A multitude of GNSS surveys has already densified or will in future densify this global reference frame, superseding the classical control networks. This process happens at local, regional or continent-wide dimensions, and has triggered a new definition and realization of national and supra-national geodetic reference systems, and strategies for integrating the existing control nets. [5]

Immediately following the development of geodetic GPS and other GNSS methods, continent-wide (supra-national) and national 3D networks were established. Although a more or less homogeneous station-coverage is generally the goal, the distances between the observation sites, in reality, vary considerably. The station distribution depends, among others, on topography and on the state of economic development, and station distances consequently range from a few ten to some 100 km and more. At least three stations per country have been often selected as a reference for further densification and for the transformation of existing control networks. The station sites are selected according to the requirements of GNSS observations (no visibility obstructions between 5° to 15° and 90° elevation, absence of multipath effects, no radio wave interference). Generally, the stations are monumented by concrete pillars, providing a forced centering for the GNSS antenna and a height reference mark. Eccentric marks are established in order to locally control horizontal position and height, and underground monuments are beneficial for the long-term preservation of the network. Existing first- and second-order control points may be used if they fulfill the GNSS requirements, otherwise, the GNSS stations should be connected to the existing control networks by local surveys. [3]

Although the strategies for establishing and maintaining these GNSS based reference networks differ, the following directions clearly can be identified:

- establishment of a large-scale (continent-wide, national) fundamental three-dimensional network by GNSS campaigns, with proper system definition and connection to the International Terrestrial Reference Frame.
- installation of a network of permanent GNSS stations.
- densification of the fundamental network by GNSS methods,
- the transformation of existing classical horizontal control network into the three-dimensional system,
- connection of the 3D-reference system to the vertical control and gravity reference systems.

Dedicated GNSS campaigns are carried out for the determination of the 3D-coordinates of the network stations, employing relative positioning. This strategy requires the inclusion of at least one reference station with coordinates given in the ITRF, but generally, all ITRF and IGS stations (or control stations of a continent-wide reference system) in the survey region are introduced as reference ("fiducial") stations. Depending on the number of stations and available GNSS receivers (two-frequency geodetic type), either all stations are observed simultaneously or the network is divided into blocks that are observed sequentially, figure (2.14). All observations made simultaneously during a given time interval are called a "session". The duration of one session is between 8 and 24 h, which permits determination of the ambiguity unknowns and a simultaneous solution for the station coordinates and tropospheric correction parameters ("multi-station" adjustment). The results of one session are highly correlated. Consequently, two or more sessions are generally carried out, leading to a total observation time of some days to one week. A "multi-session" adjustment then combines the results of several sessions. Optimization methods have been developed and may be employed for network planning and survey. [3]

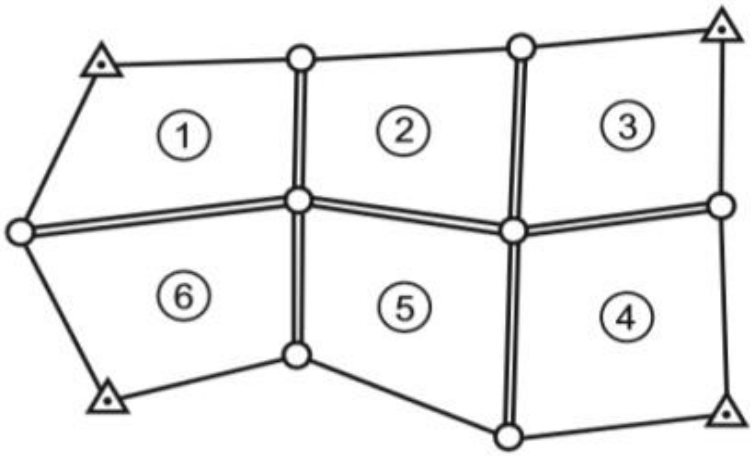

Figure (2.15): GNSS network constructed from individual blocks (principle). [5]

Following the ITRF strategy, reference epochs are defined for the final station coordinates of the fundamental networks, which may differ from the epoch of the ITRF stations introduced and from the time of the observation campaign. Consequently, reductions have to be applied which take the station velocities between the different epochs into account. [3]

Permanent GNSS networks have increasingly been established since the 1990s at regional and local scales. They consist of “active” GNSS stations, equipped with geodetic GNSS receivers that continuously track all visible GNSS satellites with a high data rate (e.g., 1 s). Station distances vary considerably, ranging from about 100 km to a few 100 km at continent-wide networks, and 30 to 100 km and more at national systems. Undisturbed visibility to the satellites is achieved by installing the antennas several m to 10 m above the ground on concrete pillars, steel grid masts, etc., or on the top of buildings. Permanent networks represent a continuous realization of the underlying supra-national or national geodetic reference system, thus serving for maintenance and for control of variations with time due to recent crustal movements. They represent a reference for all types of GNSS surveys carried out within the permanent network area, by making available the raw GNSS tracking data (code and carrier phase measurements) for the “reference” station of a “baseline”, figure (2.15). More sophisticated “Satellite Positioning Services” exploit the known geometry of the stations’ array to determine the ambiguities and to calculate baseline corrections for ionospheric, tropospheric, and orbit effects. Together with the station coordinates, this allows the application of differential GNSS methods with a single receiver. Real-time positioning with “baselines” is possible with cm-accuracy, and post-processing with long observation series may achieve a few mm precision. [5]

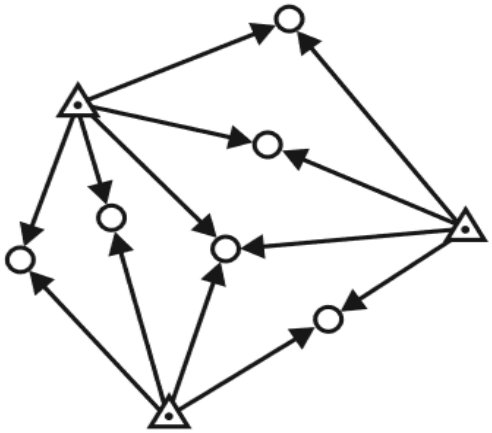

Figure (2.16): GNSS network constructed from baselines to permanent GNSS stations. [3]

After the establishment of a national 3D geodetic reference frame, relative GNSS positioning can be employed also for network densification. While the fundamental network may be constructed with station distances of several 10 km (corresponding to the first-order trigonometric points), densification nets with distances down to 10 km (former second-order triangulation) may be useful for larger countries. The relative mode again requires two or more receivers and the connection to reference stations. If a network of permanent GNSS stations as the realization of the national reference frame is available (telemetry data transfer to the users), differential GNSS methods can be applied. For short (few to 10 km) baselines, a relative cm-accuracy can be achieved in quasi-real-time after proper ambiguity solution. For longer baselines, the results are degraded by the distance-dependent errors of GNSS and have to be improved by the corrections provided by the permanent network's positioning service. [3]

With Precise Point Positioning (PPP), an alternative to the relative method of DGNSS has been developed and could also be used for the establishment of geodetic 3D control networks. This absolute method evaluates the undifferenced dual-frequency pseudo-range and carrier phase observations obtained with only one receiver, along with IGS precise orbits and satellite clock corrections in one mathematical model, for estimating station coordinates, tropospheric zenith path delays, receiver clock corrections, and ambiguities. Network adjustments (post-processing) of extended observation series (up to 24 h) deliver cm-accuracy for the position and clock corrections at the 0.1 ns level. The method can be extended by taking current corrections into account derived from a regional or local RTK

(real-time kinematic) network. This strategy allows an immediate determination of carrier-phase ambiguities and delivers quasi-real-time cm-accuracy. [5]

By connecting the 3D GNSS network to first- and second-order trigonometric points, the existing classical horizontal control networks can be transformed into the three-dimensional reference frame. A minimum of three identical points with coordinates given in both systems is required for a 7-parameter transformation, which may suffice for homogeneous networks of high precision. Additional GNSS control points are needed if the classical networks contain larger distortions; the selection of these points depends on the network peculiarities, and usually, more sophisticated transformation models will be necessary, including polynomial, least-squares, or spline approximation. In this way, the local cm-accuracy of classical networks can be kept, and the effect of the network distortions can be reduced to the order of a few cms to dm over distances of some 10 to 100 km. After the completion of the transformation to a 3D reference frame, the classical horizontal networks of lower-order generally will no longer be maintained. [4]

Space-geodetic and especially GNSS methods also give the reason for a change with respect to the definition and realization of vertical reference systems. This is due to the fact that space-based techniques allow the determination of ellipsoidal heights with an accuracy comparable with the accuracy of spirit leveling, at least at distances larger than a few ten kilometers. By combining with high-resolution global or local geoid/quasigeoid models, another method for determining gravity-field related heights thus is available. This forces the incorporation of the classical vertical control networks into the 3D reference frame. By including first-order leveling benchmarks and tide gauges in the 3D network, the differences between the ellipsoidal heights and the heights of the national height system can be determined at selected points, i.e., the geoid or quasigeoid heights. These GNSS/leveling control points allow the national height system to be fitted to a regional geoid or quasigeoid model, and they can be used to derive gravity-field related heights (orthometric heights, normal heights) for all threedimensional reference stations. The vertical datum maybe even defined by a global or regional geoid/quasigeoid model, with corresponding reductions of the heights given in the classical height system. The vertical control points now are an integrated part of the 3D reference frame, evenly distributed over the respective continent or nation and not restricted to the leveling lines. With the increasing accuracy of the geoid-resp. quasigeoid

"reduction" of GNSS heights, the application of geometric leveling will be reduced to more local problems where mm-accuracy is required.

Finally, there is a tendency to also measure absolute gravity on the primary stations of a 3D reference frame. This will lead to fundamental geodetic control networks, providing 3D geodetic coordinates, gravity potential (and related height) and gravity for a certain epoch, and (as far as possible) corresponding long-term variations with time. [3]

2.5 Gravimetric Networks

Gravity networks provide the frame for gravimetric surveys on global, regional, or local scales. They consist of gravity stations where gravity has been determined by absolute or relative methods. On a global scale, the gravity standard has been realized by the International Gravity Standardization Net 1971 (IGSN71), but absolute gravimeters now allow an independent realization. [3]

National gravimetric surveys are based on a primary or base network, which in most cases is densified by lower-order nets. The gravity base network stations should be evenly distributed over the area, with station distances varying between a few 10 km to a few 100 km depending on the size of the country. The station sites should be (as far as possible) stable with respect to geological, hydrological, and microseismic conditions. They should be permanently marked, and co-location with geodetic base-stations is advisable. Eccenter sites may serve for securing the central station and for controlling local height and mass changes. Horizontal position and height of the gravity stations should be determined with m- and mm- to cm-accuracy, respectively. Subsequent gravimetric densification networks generally are co-located with horizontal and vertical control nets. [3]

Absolute gravimeters, figure (2.17) generally are employed nowadays for the establishment of gravity base networks, partly in combination with relative gravity meters. Densification networks are observed primarily with relative instruments. Relative gravimeters, figure (2.18) need to be calibrated, and repeated measurements are necessary in order to determine the instrumental drift. The use of several instruments reduces residual systematic effects. Relative gravimetry requires at least one absolute station in order to derive the gravity “datum”, and a calibration line for the control and improvement of the calibration factor. The establishment of gravity networks for geophysical and geodynamic investigations

follows the same rules, but the distribution of the gravity stations is then determined by the geological structures or the geodynamic processes to be investigated. [5]

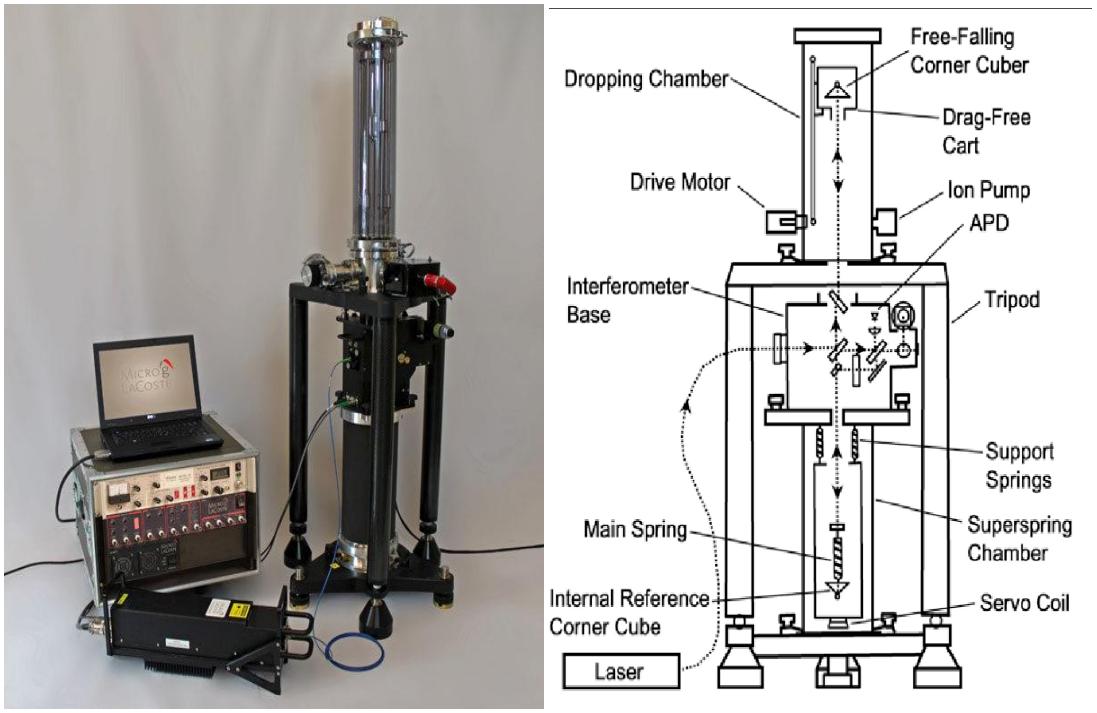

Figure (2.17): Absolute gravimeters.

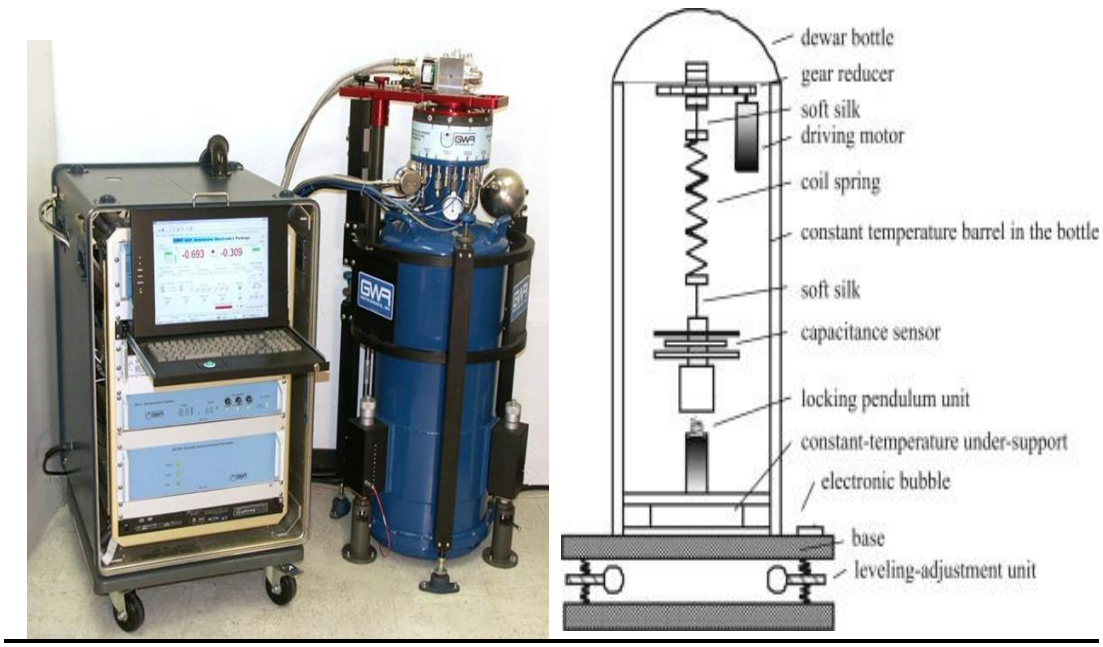

Figure (2.18): Relative gravimeter.

The accuracy of primary gravity networks, established by absolute gravimeters or by a combination of absolute and relative gravimetry, is about 0.05 μm s^2 to 0.1 μm s^2; densification networks may be accurate to 0.1… 0.5 μm s^2.

Gravity measurements on the national scale started in the second half of the nineteenth century, triggered by growing demands from geodesy and geophysics. In the twentieth century, exploration geophysics and physical geodesy (geoid determination) became strong drivers for denser gravity field surveying, based on accurate and reliable gravity reference networks. These demands led in many countries to the establishment of gravity base networks, which continuously improved through progress in technology. [5]

Figure (2.19): Primary gravity net (red circles) of Germany. [3]

Chapter Three:

Global and local gravity Geoid modeling

3.1 Introduction

3.2 The gravity field of the Earth

3.3 The local potential modeling

3.4 Integrated Geodesy

3.5 State of the art in the gravity field modeling

Global and local gravity Geoid modeling

3.1 Introduction

This chapter presents the potential of the Earth and its applications based on Newton's Law of Attraction and explains the relationship between the potential and the force of attraction. This chapter explains the Laplace equation solution using the Spherical Harmonics (SH) model, which is applied to the gravity field modeling of the earth. It also explains the relationship between the actual gravitational field and the natural gravitational field of the earth is, where an abnormal gravitational field is introduced .[8]

The common way to represent the potential of the Earth is by Spherical Harmonics, but the related methods require global modeling. There is always a need to model the potential by other methods with local support for national and regional needs. Here, some of the common methods for local modeling of the potential of the Earth are discussed. Such suitable methods are the Stokes integral for gravimetric geoid modeling, the least-squares collocation and the Digital Finite Elements Height Reference Surface (DFHRF) developed at the Karlsruhe University of Applied Sciences. [8]

The so-called Integrated Geodesy principle, where a combination of different data types of observations $l = l(\vec{x}, W(\vec{x}, p))$ are modeled in the gravity and geometry space, are also briefly discussed. In addition, the state-of-the-art of the latest global and local geoid and gravity models is presented. [8]

3.2 The gravity field of the Earth

Depending on Newton's law of attraction, the force of attraction between two mass m_1 and m_2 (kg) separated by a specific distance l(m) is calculated. The attraction force F reads:

$$\vec{F} = G\frac{m_1 m_2}{l^2} \tag{3-1}$$

To study how a mass *m* attracts other masses, assume that the attracted masses to be a unit mass ($m_1 = 1$). The force attracting the unit mass at point $P(X, Y, Z)$ by the mass *m* at $P_0(X_0, Y_0, Z_0)$ separated by a distance *l* is:

$$F = G\frac{m}{l^2} \tag{3-2}$$

The force $\vec{F}$ is represented by a vector from P_0 to P. The vector of the gravitational force $\vec{F}$ can be defined by its magnitude $\vec{F}$ and 3D components of the unit vector F is given by:

$$\vec{F} = \begin{bmatrix} F_X \\ F_Y \\ F_Z \end{bmatrix} = -F \begin{bmatrix} (X - X_0)/l \\ (Y - Y_0)/l \\ (Z - Z_0)/l \end{bmatrix} = -\frac{GM}{l^2} \begin{bmatrix} (X - X_0)/l \\ (Y - Y_0)/l \\ (Z - Z_0)/l \end{bmatrix} \quad (3\text{-}3)$$

The gravitational potential is a conservative, which satisfies the Laplace differential equation outside the Earth. A scalar force-generating potential exists. This function is called the gravitational potential V (X, Y, Z), where V reads:

$$V(X, Y, Z) = \frac{GM}{l} \quad (3\text{-}4)$$

The unit mass related force vector $\vec{F}$ in equation (3-3) can be rewritten in terms of V as follows:

$$\vec{F} = grad(V) \quad (3\text{-}5a)$$

$$\vec{F} = \begin{bmatrix} F_X \\ F_Y \\ F_Z \end{bmatrix} = \begin{bmatrix} \frac{\partial V}{\partial X} \\ \frac{\partial V}{\partial Y} \\ \frac{\partial V}{\partial Z} \end{bmatrix} \quad (3\text{-}5b)$$

Assuming a system of point masses $m_1, m_2, \ldots, m_n$ are attracting the point P, and separated from the point P by distances $l_1, l_2, .., l_n$, then the gravitational potential V is the summation of all single potentials. The total gravitational potential is:

$$V(X, Y, Z) = \sum_{i=1}^{n} V_i = \sum_{i=1}^{n} \frac{GM_i}{l_i} \quad (3\text{-}6)$$

If the point P is influenced by a solid body with a volume v and a density of ρ (X, Y, Z), then the potential V is calculated by a superimposing infinite number of point masses dm. The point mass can be calculated by the volume of point mass dv and the density ρ, reading:

$$dm = \rho dv \quad (3\text{-}7)$$

The total gravitational potential by the solid body is calculated by the integration over the whole volume of the solid body. V is given by:

$$V = \int dV = G \iiint_V \frac{\rho(X,Y,Z)dv}{l} \quad (3\text{-}8)$$

3.2.1 Laplace differential equation and Spherical Harmonics (SH)

For a function V(X, Y, Z), the Laplace equation for this function is the Laplace operator Δ(.)=0 and reads:

$$\Delta(V) \equiv \frac{\partial^2 V}{\partial X^2} + \frac{\partial^2 V}{\partial Y^2} + \frac{\partial^2 V}{\partial Z^2} = 0 \tag{3-9}$$

Using spherical coordinates (r,ϕ,λ) as defined in figure (3.1), Laplace's equation can be transformed to:

$$r^2 \frac{\partial^2 V}{\partial r^2} + 2r \frac{\partial V}{\partial r} + \frac{\partial^2 V}{\partial \overline{\phi}^2} - \tan\phi \frac{\partial V}{\partial \overline{\phi}} + \frac{\partial^2 V}{cos^2 \overline{\phi} \partial \lambda^2} \tag{3-10}$$

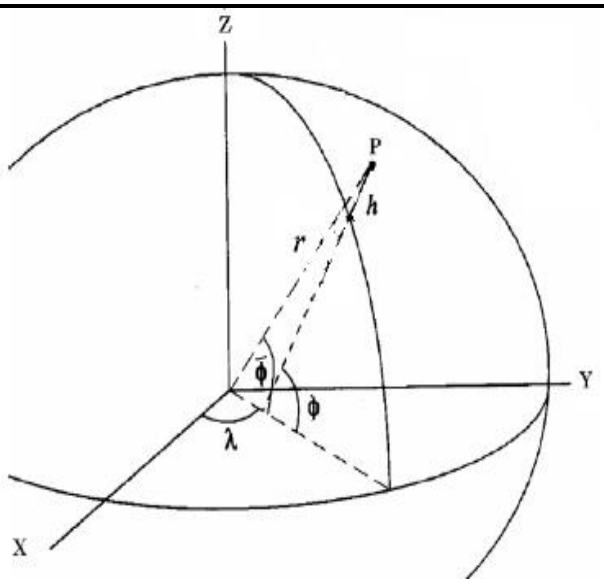

Figure (3.1): Geographic coordinates (λ,ϕ, h)and the spherical coordinates(r, λ, $\overline{\phi}$). [8]

Assuming that the density ρ is constant (ρ) is given the value of the average density of the Earth) and *dv* is the same for all elements, then only *l* is changing for each element. The Laplace operator for the gravitational potential in equation (3-8) is given by:

$$\Delta(V) = \Delta\left(G \iiint_v \rho dv\right) = G \iiint_v \Delta\left(\frac{1}{l}\right) \rho dv = 0 \tag{3-11}$$

As $\Delta\left(\frac{1}{l}\right) = 0$, V is a harmonic function. The solution of Laplace's equation is found by separating the variables (r, λ and $\overline{\phi}$) using the substitution in equation (3-12), reading:

$$V\left(r, \overline{\phi}, \lambda\right) = f_1(r) f_2\left(\overline{\phi}\right) f_3(\lambda) \tag{3-12a}$$

$$f_1(r) = \frac{1}{r^{n+1}} \qquad \text{n=0,1,2,...} \tag{3-12b}$$

$$f_2(\overline{\phi}) = P_{nm}\sin(\overline{\phi}) \qquad \text{n=0,1,2,… and m=0,1,2,…,n-1,n} \tag{3-12c}$$

$$f_3(\lambda) = \cos m\lambda \;\; or \;\; \sin m\lambda \qquad \text{m=0,1,2,…n-1,n} \tag{3-12d}$$

In equation (3-12), $P_{nm} = (\sin\overline{\phi})$ are the Legendre functions of degree n and order m. Assuming $\sin\overline{\phi} = t$, the Legendre function is generally defined by the differential formula in equation (3-13):

$$P_{nm}(t) = \frac{1}{2^n n!}(1-t)^{m/2}\frac{d^m P_n(t)}{dt^m}(t^2-1)^n \tag{3-13}$$

As the differential equation (3-10) is linear, for each integer n there is a solution. The summation of all solutions is also a solution for Laplace's equation $\Delta V = 0$. The potential V can be written in terms of surface Spherical Harmonics (SH) in equation (3-15).

$$V(r,\overline{\phi},\lambda) = \sum_{n=0}^{\infty}\frac{1}{r^{n+1}}\sum_{m=-n}^{n} A_{nm}Y_{nm}(\overline{\phi},\lambda) \tag{3-14}$$

$$\mathrm{Y_{nm}}(\overline{\phi},\lambda) = \begin{cases} \cos \mathrm{m}\lambda \mathrm{P_{n|m|}}\left(\sin\overline{\phi}\right) & , \mathrm{m} \le 0 \\ \sin \mathrm{m}\lambda \mathrm{P_{nm}}\left(\sin\overline{\phi}\right) & , \mathrm{m} > 0 \end{cases} \tag{3-15a}$$

$$A_{nm} = \begin{cases} a_{nm} & , m \le 0 \\ b_{nm} & , m > 0 \end{cases} \tag{3-15b}$$

Equation (3-14) can be reformulated as double summation. In this case V reads:

$$\mathrm{V}(\mathrm{r},\overline{\phi},\lambda) = \sum_{\mathrm{n=0}}^{\infty}\frac{1}{\mathrm{r^{n+1}}}\sum_{\mathrm{m=0}}^{\mathrm{n}}(\mathrm{a_{nm}}\cos \mathrm{m}\lambda + \mathrm{b_{nm}}\sin \mathrm{m}\lambda)\mathrm{P_{nm}}\sin(\overline{\phi}) \tag{3-16}$$

3.2.2 The normalized SH

As shown above, the gravitational potential V satisfies the Laplace equation. In equation (3-14), V was modeled to solve the Laplace equation in terms of SH. When higher degrees and orders Legendre functions $P_{nm}(t)$ are calculated, instability problems appear in the calculations. To avoid these issues, a normalized form of equation (3-14) is introduced in equation (3-17) using the normalized Legendre functions $\overline{P}_{nm}(t)$. [8]

$$V(r,\overline{\phi},\lambda) = \sum_{n=0}^{\infty}\frac{1}{r^{n+1}}\sum_{m=-n}^{n}\overline{A}_{nm}\overline{Y}_{nm}(\overline{\phi},\lambda) \tag{3-17a}$$

$$\overline{Y}_{nm}(\overline{\phi},\lambda) = f_{nm}Y_{nm}(\overline{\phi},\lambda) \tag{3-17b}$$

$$\overline{P}_{nm}(t) = f_{nm}P_{nm}(t) \tag{3-17c}$$

$$\overline{A}_{nm} = \frac{A_{nm}}{f_{nm}} \tag{3-17d}$$

Finally, the potential V reads:

$$V(r,\overline{\phi},\lambda) = \sum_{n=0}^{\infty}\frac{1}{r^{n+1}}\sum_{m=0}^{n}(\overline{a}_{nm}\cos m\lambda + \overline{b}_{nm}\sin m\lambda)\overline{P}_{nm}(\sin\overline{\phi}) \tag{3-18}$$

The normalizing function f_{nm} in equation (3-17) reads:

$$f_{nm} = \begin{cases}\sqrt{2n+1} & ,m = 0\\ 2(2n+1)\frac{(n-m)!}{(n+m)!} & ,m \neq 0\end{cases} \tag{3-19}$$

The coefficients $\overline{a}_{nm}$ and $\overline{b}_{nm}$ are constants, which have to be determined. They are generally called the spherical harmonic coefficients. [8]

3.2.3 The normalized Legendre functions

Substituting the normalizing function f_{nm} in equation (3-19) in the recursive formula of Legendre function P_{nm} in equation (3-13), the fully normalized Legendre function in equation (3-20) is realized. $\overline{P}_{nm}(\sin\overline{\phi})$ is the fully normalized associated Legendre function. $\overline{P}_{nm}(\sin\overline{\phi})$ can be calculated by the recursive formulas (3-20), with the abbreviations $t = \cos\overline{\phi}$ and $u = \cos\overline{\phi}$ as follows:

$$\overline{P}_{n,m} = a_{nm}t\overline{P}_{n-1,m} - b_{nm}\overline{P}_{n-2,m} \tag{3-20a}$$

$$a_{nm} = \sqrt{\frac{(2n-1)(2n+1)}{(n-m)(n+m)}} \tag{3-20b}$$

$$b_{nm} = \sqrt{\frac{(2n+1)(n+m-1)(n-m-1)}{(n-m)(n+m)(2n-3)}} \tag{3-20c}$$

$$\overline{P}_{0,0} = 1 \quad , \quad \overline{P}_{1,0} = \sqrt{3}t \quad , \quad P_{1,1} = \sqrt{3}u \tag{3-20d}$$

If n=m, then $\overline{P}_{n,m}$ reads:

$$\overline{P}_{m,m} = u\sqrt{\frac{2m+1}{2m}}P_{m-1,m-1} \tag{3-20e}$$

The first derivative of the fully normalized Legendre polynomial $\frac{\partial \overline{P}_{n,m}}{\partial \phi}$ can be calculated using the calculated values of the recursive formulas in equations (3-20). There is no need for new recursive formulas to calculate the derivatives of the Legendre functions; the calculated value of the Legendre polynomial $\overline{P}_{nm}$ can be applied directly to calculate the derivatives of the Legendre polynomial, reading: [8]

$$\frac{\partial \overline{P}_{n,m}}{\partial \overline{\phi}} = \frac{1}{u}\left(n\ t\ \overline{P}_{n,m}\sqrt{\frac{(n^2-m^2)(2n+1)}{2n-1}}\overline{P}_{n-1,m}\right) \qquad \text{for n>m} \tag{3-21a}$$

$$\frac{\partial \overline{P}_{n,m}}{\partial \overline{\phi}} = \frac{1}{u}\ n\ t\ \overline{P}_{n,m} \qquad \text{for n = m} \tag{3-21b}$$

3.2.4 Harmonic expansion of the Earth gravitational potential

Equations (3-17) and (3-18) are used to evaluate the gravitational potential V at a point P(r, $\overline{\phi}$, λ), attracted by the solid body of the Earth. Equations (3-20a) to (3-20e) are used to calculate the Legendre functions. The coefficients (a_{nm}, b_{nm}) in equation (3-18) can be used to evaluate the gravitational potential V at the point P created by the mass of the Earth. Depending on the orthogonality conditions, the coefficients a_{nm} and b_{nm} are given by [8]

$$a_{nm} = \frac{G}{2n+1}\iiint_v (r')^n \cos m\lambda'\ \overline{P}_{nm}\left(\sin\overline{\phi'}\right)\rho\ dv \tag{3-22a}$$

$$b_{nm} = \frac{G}{2n+1}\iiint_v (r')^n \sin m\lambda'\ \overline{P}_{nm}\left(\sin\overline{\phi'}\right)\rho\ dv \tag{3-22b}$$

By substituting m=0 and n=0, we find $\overline{b}_{00} = 0$, and $\overline{a}_{00} = 0$ is given by:

$$\overline{a}_{00} = G\iiint_v p\ dv = GM \tag{3-23}$$

Substituting $\overline{a}_{00}$ in equation (3-18) results in:

$$V_{00} = \frac{GM}{r} \tag{3-24}$$

To find $\overline{a}_{10}$, $\overline{a}_{11}$,and $\overline{b}_{11}$, we have:

$$\overline{a}_{10} = \frac{G}{3} \iiint_v r' \sqrt{3} \sin \overline{\phi'}\, dm \tag{3-25a}$$

$$\overline{a}_{11} = \frac{G}{3} \iiint_v r' \cos \lambda' \sqrt{3} \cos \overline{\phi'}\, dm \tag{3-25b}$$

$$\overline{b}_{11} = \frac{G}{3} \iiint_v r' \cos \lambda' \sqrt{3} \cos \overline{\phi'}\, dm \tag{3-25c}$$

Geographic coordinates of the point element can be transformed into the Cartesian coordinates using equations (3-26a) to (3-26c).

$$r' \sin \phi' = z' \tag{3-26a}$$

$$r' \cos \phi' \cos \lambda' = x' \tag{3-26b}$$

$$r' \cos \phi' \sin \lambda' = y' \tag{3-26c}$$

Then $\overline{a}_{10}$, $\overline{a}_{11}$, and $\overline{b}_{11}$ read:

$$\overline{a}_{10} = \frac{G}{\sqrt{3}} \iiint z'\, dm \tag{3-27a}$$

$$\overline{a}_{11} = \frac{G}{\sqrt{3}} \iiint x' dm \tag{3-27b}$$

$$\overline{b}_{11} = \frac{G}{\sqrt{3}} \iiint y'\, dm \tag{3-27c}$$

In mechanics, the coordinates of the center of mass of a rigid body are:

$$x_0 = \frac{1}{M} \iiint_v x'\, dm \tag{3-28a}$$

$$y_0 = \frac{1}{M} \iiint_v y'\, dm \tag{3-28b}$$

$$z_0 = \frac{1}{M} \iiint_v z'\, dm \tag{3-28c}$$

Inserting equations (3-28a) to (3-29c) in equations (3-27a) to (3-28c) results in:

$$\overline{a}_{10} = \frac{GM}{\sqrt{3}} z_0 \tag{3-29a}$$

$$\overline{a}_{11} = \frac{GM}{\sqrt{3}} x_0 \tag{3-29b}$$

$$\overline{b}_{11} = \frac{Gm}{\sqrt{3}} y_0 \tag{3-29c}$$

For a properly chosen reference frame, the origin of the coordinate system coincides with the center of mass of the Earth. Therefore, x_0, y_0, and z_0 are equal to zero, meaning that the related coefficients are zero as well. [8]

$$a_{10} = a_{11} = b_{10} = b_{11} = 0 \tag{3-30}$$

Inserting equation (3-24) and (3-30) in equation (3-25) results in:

$$V(r, \overline{\phi}, \lambda) = \frac{GM}{r} + \sum_{n=2}^{\infty} \frac{1}{r^{n+1}} \sum_{m=0}^{n} (\overline{a}_{nm} \cos m\lambda + \overline{b}_{nm} \sin m\lambda) \overline{P}_{nm}(\sin \overline{\phi}) \tag{3-31}$$

The spherical harmonic coefficients $\overline{a}_{nm}$ and $\overline{b}_{nm}$ in equation (3-31) can be normalized using the gravitational constant GM and the semimajor axis of the reference ellipsoid a as shown in equations (3-32a) and (3-32b) to get new normalized coefficients $\overline{C}_{nm}$ and $\overline{S}_{nm}$.

$$\overline{C}_{nm} = \frac{1}{a^n GM} \overline{a}_{nm} \tag{3-32a}$$

$$\overline{S}_{nm} = \frac{1}{a^n GM} \overline{b}_{nm} \tag{3-32b}$$

Inserting (3-32) in equation (3-31) results in equation (3-33a) or equivalently (3-33b).

$$V(r, \overline{\phi}, \lambda) = \frac{GM}{r} + \frac{GM}{a} \sum_{n=2}^{\infty} \left(\frac{a}{r}\right)^{n+1} \sum_{m=0}^{n} (\overline{C}_{nm} \cos m\lambda + \overline{S}_{nm} \sin m\lambda) \overline{P}_{nm}(\sin \overline{\phi}) \tag{3-33a}$$

$$V(r, \overline{\phi}, \lambda) = \frac{GM}{r} + \frac{GM}{r} \sum_{n=2}^{\infty} \left(\frac{a}{r}\right)^{n} \sum_{m=0}^{n} (\overline{C}_{nm} \cos m\lambda + \overline{S}_{nm} \sin m\lambda) \overline{P}_{nm}(\sin \overline{\phi}) \tag{3-33b}$$

3.2.5 Derivatives of the potential of the Earth

A point P on the Earth's surface is subjected to two types of acceleration. The first type is the gravitational acceleration part $\vec{g}_1$ due to the Earth's mass M. The second type $\vec{z}$ is the centrifugal acceleration due to the Earth's rotation. The total acceleration $\vec{g}$ is the vector summation of both gravitational and centrifugal accelerations, which represent the actual gravity vector:

$$\vec{g} = \vec{g}_1 + \vec{z} \tag{3-34}$$

The relationship between the accelerations in equation (3-34) and their related potential is given in equation (3-35). The total gravity potential W, created by the total acceleration,$\vec{g}$, is

the summation of the gravitational potential V and the centrifugal potential Ω. This total gravity potential is given by:

$$W = V + \Omega \tag{3-35}$$

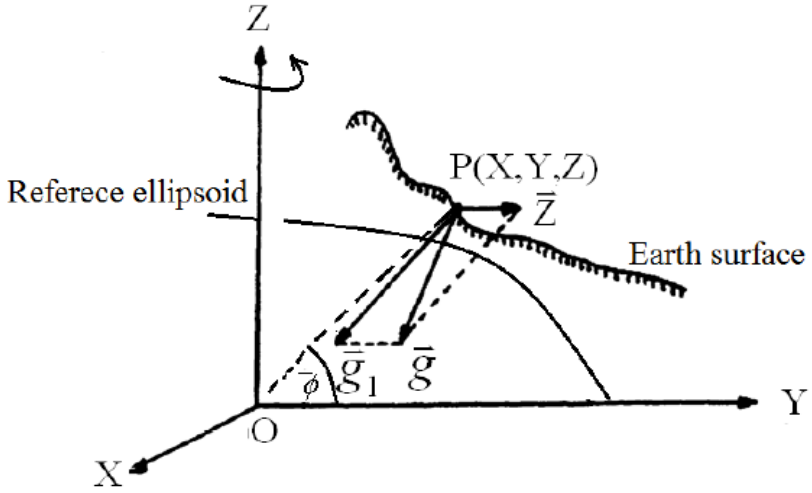

Figure (3.2): The gravitational and centrifugal accelerations of the Earth. [8]

The centrifugal potential is caused by rotation of the Earth around its minor axis. The centrifugal acceleration vector will, therefore, have only two components in the X and Y directions. As the angular velocity ω of the Earth around its minor axis is $0.7292115 \times 10^{-4} s^{-1}$ as defined by the GRS80, the centrifugal potential reads:

$$\Omega = 0.5\omega^2 r^2 \cos\overline{\phi} = \frac{1}{2}\omega^2(X^2 + Y^2) \tag{3-36}$$

Its related centrifugal acceleration vector and magnitude are:

$$\vec{z} = grad(\Omega) = \begin{bmatrix} \omega^2 X \\ \omega^2 Y \\ 0 \end{bmatrix} = \begin{bmatrix} \omega^2 r \cos\overline{\phi}\cos\lambda \\ \omega^2 r \cos\overline{\phi}\sin\lambda \\ 0 \end{bmatrix} \tag{3-37a}$$

$$z = |\vec{z}\,| = \sqrt{\left(\frac{\partial\Omega}{\partial X}\right)^2 + \left(\frac{\partial\Omega}{\partial Y}\right)^2 + \left(\frac{\partial\Omega}{\partial Z}\right)^2} = \omega^2\sqrt{X^2 + Y^2} = \omega^2 r\cos\overline{\phi} \tag{3-37b}$$

The total gravity vector is the gradient of the gravity potential W ($\vec{g} = grad\ W$). This can be formulated in equation (3-38) in 3D-cartesian coordinates.

$$\vec{g} = \left[\frac{\partial W}{\partial X} \quad \frac{\partial W}{\partial Y} \quad \frac{\partial W}{\partial Z}\right] \tag{3-38}$$

In spherical coordinates, equation (3-38) reads:

$$\vec{\mathrm{g}} = \left[\frac{\partial W}{\partial r} \quad \frac{\partial W}{r\cos\overline{\phi}\partial\lambda} \quad \frac{\partial W}{r\partial\overline{\phi}}\right] \tag{3-39}$$

Substituting equation (3-35) in equation (3-39) results in:

$$\vec{\mathrm{g}} = \left[\frac{\partial(V+\Omega)}{\partial r} \quad \frac{\partial(V+\Omega)}{r\cos\overline{\phi}\partial\lambda} \quad \frac{\partial(V+\Omega)}{r\partial\overline{\phi}}\right] \tag{3-40}$$

The derivatives of the gravitational potential V in equation (3-40) are given by:

$$\frac{\partial V}{\partial r} = \frac{GM}{r^2} - \frac{GM}{r^2}\sum_{\mathrm{n=2}}^{\max}{}_{\mathrm{n}}\left(\frac{\mathrm{a}}{\mathrm{r}}\right)^{\mathrm{n}}(\mathrm{n}+1)\sum_{m=0}^{n}\left(\overline{C}_{n,m}\cos(m\lambda) + \overline{S}_{n,m}\sin(m\lambda)\right)\overline{P}_{n,m}\left(\sin\overline{\phi}\right) \tag{3-41a}$$

$$\frac{\partial V}{\partial \lambda} = \frac{GM}{r}\sum_{n=2}^{\max}{}_{n}\left(\frac{a}{r}\right)^{n}\sum_{m=0}^{n} m.\left(\overline{S}_{n,m}\cos(m\lambda) - \overline{C}_{n,m}\sin(m\lambda)\right)\overline{P}_{n,m}\left(\sin\overline{\phi}\right) \tag{3-41b}$$

$$\frac{\partial V}{\partial \lambda} = \frac{GM}{r}\sum_{n=2}^{\max}{}_{n}\left(\frac{a}{r}\right)^{n}\sum_{m=0}^{n} m.\left(\overline{C}_{n,m}\cos(m\lambda) + \overline{S}_{n,m}\sin(m\lambda)\right)\frac{\partial\overline{P}_{n,m}}{\partial\overline{\phi}} \tag{3-41c}$$

The derivatives of the centrifugal potential read:

$$\frac{\partial\Omega}{\partial r} = \omega^2\cos^2\overline{\phi} \tag{3-42a}$$

$$\frac{\partial\Omega}{\partial\lambda} = 0 \tag{3-42b}$$

$$\frac{\partial\Omega}{\partial\overline{\phi}} = \omega^2 r^2\cos\overline{\phi}\sin\overline{\phi} \tag{3-42c}$$

The magnitude of gravity reads:

$$\mathrm{g} = |\vec{\mathrm{g}}| = \sqrt{\left(\frac{\partial(V+\Omega)}{\partial r}\right)^2 + \left(\frac{\partial(V+\Omega)}{r\cos\overline{\phi}\partial\lambda}\right)^2 + \left(\frac{\partial(V+\Omega)}{r\partial\overline{\phi}}\right)^2} \tag{3-43}$$

By using the SH formulas, it is easy to derive any other functional quantities related to the potential. The most referred functional quantities in equation (3-44) are the gravity vector $\vec{\mathrm{g}}_{LGV\_Sphere}$ in spherical-LGV, $\vec{\mathrm{g}}_{LGV}$ in LGV, quasigeoid heights (height anomalies) ζ, the geoid height N, and deflections of the vertical in the east and north directions (η,ζ). [8]

$$\mathrm{g}^{LGV\_Sphere} = \left[\frac{\partial W}{\partial r} \quad \frac{\partial W}{r\cos\overline{\varphi}\partial\lambda} \quad \frac{\partial W}{r\partial\overline{\varphi}}\right] \text{ and } \mathrm{g}^{LGV\_Ellipsoid} = R(\lambda,\varphi)_e^n.\begin{bmatrix}W_x\\W_y\\W_z\end{bmatrix} \tag{3-44a}$$

Where the absolute value g at a position P(x,y,z) is both the same. The following quantities (3-44b) to (3-44e) are referring to the ellipsoid, a modern ellipsoidal georeferencing, and the respective reference gravity field (at present GRS80):

$$\zeta = \frac{T}{\gamma_Q} \tag{3-44b}$$

$$N = \frac{T}{\gamma_Q} + \frac{\overline{g}-\overline{\gamma}}{\overline{\gamma}} H_p = \zeta + \frac{\overline{g}-\overline{\gamma}}{\overline{\gamma}} H_p \tag{3-44c}$$

$$\xi = \frac{\partial N}{\partial s_{North}} = -\frac{1}{\gamma_Q (M+h)} \frac{\partial T}{\partial \phi} \tag{3-44d}$$

$$\eta = \frac{\partial N}{\partial s_{East}} = -\frac{1}{\gamma_Q (N+h)\cos\phi} \frac{\partial T}{\partial \lambda} \tag{3-44e}$$

With $\overline{\gamma}$ and $\overline{g}$ the integrated quantities of the reference and the true gravity field (3-44a), respectively, along the plumb line (practically and without loss of validity computed along the ellipsoidal normal), are introduced. T is a disturbing potential. γ_Q is the ellipsoidal normal gravity for a point Q on the so-called telluride with the same latitude and longitude as the calculation point and an ellipsoidal height of $h_Q = H^*{}_p = h_p - \zeta$. The telluride is defined as the surface whose normal potential U_Q is equal to the actual potential at point W_P see figure (3.3). The telluride is not an equipotential surface. s_{North} and s_{East} are the differential distance elements towards North and East, respectively. M and N are the ellipsoidal radii of curvature in the directions of longitude and latitude, respectively. The geoid (N) coincides with the mean sea level and was earlier used height reference surface by measuring the tide gauges at the coast of a country. [8]

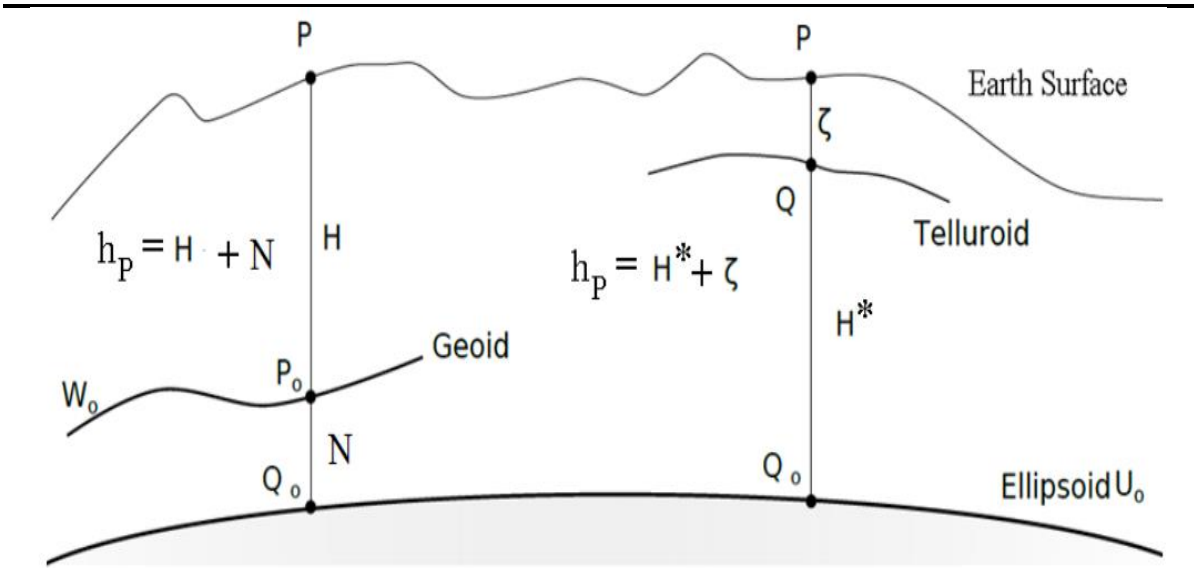

Figure (3.3): Height anomaly ζ vs. geoid height N. [8]

3.2.6 The spherical harmonic expansion of the Earth's gravity field

The common way of representing the gravitational potential V in a global model is to use the SH. Presently, there are many global gravity potential field models available from various sources and with different spatial resolutions. The International Center for Global Gravity Models (ICGEM) provides access to the various satellite-only or combined models on behalf of the International Association of Geodesy. Examples of these models are shown in table (3.1). [8]

Table (3.1): Some of the common global gravity models with their data sources [8]

Model	Year	Degree	Data
EIGEN06c	2011	1420	S(GOCE,GRACE,LAGEOS),G,A
EIGEN051c	2010	359	S(GRACE, CHAMP),G,A
EIGEN05c	2008	360	S(GRACE,LAGEOS),G,A
EGM2008	2008	2190	S(GRACE),G,A
EIGEN-GL04c	2006	360	S(GRACE,LAGEOS),G,A
GGM02c	2004	200	S(GRACE),G,A
EIGEN-CG01c	2004	360	S(CHAMP,GRACE),G,A
PGM2000A	2000	360	S,G,A
EGM96	1996	360	S,G,A

Data: S=Satellite gravity data, G = Gravity data, A = Altimetry data

The calculation of the SH coefficients can only be solved by means of global data coverage. This could only be achieved after the first geodetic satellite missions (like the LAGEOS, GRACE, GOCE and CHAMP missions). The satellite missions are utilizing different types of measurement principles. The LAGEOS satellites apply the principle of Satellite Laser Ranging (SLR), while the CHAMP mission uses the principle of Satellite-to-Satellite tracking in highlow mode, where the residual gravity accelerations are additionally measured by means of an accelerometer. The GRACE Satellite mission uses the principle of Satellite-to-Satellite tracking in low-low mode, where the gravity differences between two satellites separated by hundreds of kilometers are observed. The most modern GOCE mission uses the principle of gravity gradiometry using a group of accelerometers fixed on the three axes of the satellite. The combination of satellite observations with terrestrial measurements led to the combined gravity models (e.g. EGM98A, EGM96, EIGEN06c, and EGM2008).

The SH can be calculated by two methods: the first is the integration method that keeps the orthogonality conditions of the SH, and the second is the least-squares estimation. [8]

The integration methods have several problems. One is that the data have to be downward continued to the zero levels (geoid) resulting in the so-called surface SH; the other is that the weighting of observations of different sources is not possible. The integration formulas to calculate the spherical harmonic coefficients using the gravity anomalies Δg and the geoid heights N are given by:

$$\begin{Bmatrix} \overline{C}_{nm} \\ \overline{S}_{nm} \end{Bmatrix} = \frac{1}{4\pi GM} \iint_{\sigma} r\gamma \left(\frac{r}{a}\right)^{n} N\overline{P}_{nm} \begin{Bmatrix} \cos m\lambda \\ \sin m\lambda \end{Bmatrix} d\sigma \tag{3-45a}$$

$$\begin{Bmatrix} \overline{C}_{nm} \\ \overline{S}_{nm} \end{Bmatrix} = \frac{1}{4\pi GM} \iint_{\sigma} \frac{r^2}{n-1} \left(\frac{r}{a}\right)^{n} \Delta g\overline{P}_{nm} \begin{Bmatrix} \cos m \\ \sin m \end{Bmatrix} d\sigma \tag{3-45b}$$

In the least-squares solution, the introduction of the variance and covariance matrices is possible for each group of data or for any single observation.

The solutions have always been applied in two modes: the satellite-only models and the combined models. The advantage of satellite-only methods is that they use direct gravity or a potential function as input without the need for any reductions or corrections. On the other hand, there is always mixing related to the terrestrial gravity data in the combined methods. Sometimes the terrestrial gravity data are free-air gravity and sometimes Bouguer anomalies. The geoid/quasigeoid heights at the height fitting points may also be related to different vertical datums. They can also be in different types of heights like the orthometric, normal or dynamic heights. For these reasons, it is more desirable to have the satellite-only models alone without the combination of terrestrial data. [8]

The satellite-only models use data measured over long time periods. This provides information about time-dependent changes of the Earth-like plate tectonics, ocean circulation, ice mass variations, tides, etc. Each of these time-dependent effects will affect the measured gravity values. For these reasons, they are suitable to be used in defining the global physical reference surface. [8]

The satellite-only methods have a limited resolution which leads to lower degree and order of the SH model. In addition, there are always some gaps in the data, especially near the poles, but the representation of the quasigeoid requires high degrees and orders with global

coverage of data. For these reasons, terrestrial data are required to achieve higher accuracy in the combined models. [8]

3.3 The local potential modeling

Here, different principles of local potential and gravity modeling are introduced. The methods discussed in this chapter are the Stokes formula including the remove-restore method, GNSS/Leveling, the Finite Elements Methods, and the Least Squares Collocation. There are many other principles available, like the astrogeodetic methods,…, etc. [8]

3.3.1 Stokes formula and remove-restore method

The Stokes formula (Stokes Integral), derived by Stokes (1849), is one of the most commonly used methods for the computation of highly accurate geoid models by means of a grid of surface gravity anomalies Δg. Here, Δg is the difference between the real gravity on the geoid surface observation and the g_p ellipsoidal normal gravity on the ellipsoid surface γ_Q. The gravity anomaly Δg reduced to geoid level to get Δg_0 to calculate the geoid using free correction and terrain corrections. Where Δg and Δg_0 read: [8]

$$\Delta g = g_p - \gamma_Q \tag{3-46a}$$

$$\Delta g = g_{p0} - \gamma_{Q0} \tag{3-46b}$$

The point P, P_0, Q, and Q_0 are explained in figure (3.3). The Stokes formula reads:

$$N = \frac{a}{4\pi\gamma_m} \iint_\sigma S(\psi)\Delta g \, d\sigma \tag{3-47}$$

Here, ***a*** is the semimajor axis of the reference ellipsoid, The Stokes function S(ψ) is given by:

$$S(\psi) = \sum_{n=2}^{\infty} \frac{2n+1}{n-1} P_n(\psi) \tag{3-48}$$

In equation (3-47), ψ is the spherical distance between the point of interest and a grid point with given gravity anomaly Δg. $P_n(\psi)$ is the zero-order Legendre function related to ψ. For the implementation of Stokes integral, the scattered gravity anomalies gravity points have to be gridded over the complete Earth's surface to enable calculation of the geoid heights. [8]

As the Stokes formula has to be applied globally in principle, an enhancement to this formula has commonly been used to model the geoid height locally using the long-

wavelength effect, which is introduced by the available global gravity models. In addition, the combination of the global models with dense gravity data and high-resolution Digital Terrain Models (DTM) leads to the so-called remove-restore technique. [8]

In the remove-restore technique, the gravity anomaly grid points Δg are reduced by the gravity anomalies computed from a global gravity model Δg_{global}. The effect of the terrain then has to be reduced Δg_{DTM}. The resultant gravity anomalies (residual anomalies) $\Delta g_{residual}$ are applied in the Stokes formula to obtain the residual geoid heights $\Delta N_{residual}$. The final geoid height is given by:

$$N = N_{global} + \Delta N_{residual} + \Delta N_{DTM} \tag{3-49}$$

The use of the remove-restore method enables the application of Stokes formulas over smaller areas. This makes it possible to work with planar approximations, enabling the application of the FFT. The use of the Stokes formula is not possible by the combination of different data types with different accuracy measures. Furthermore, a grid of gravity anomalies must always be used. In this way, the single gravity observations cannot be statistically weighted and tested according to the measurement accuracy. [8]

3.3.2 GNSS/Leveling

The GNSS/GPS leveling can be directly used in the defining the eight reference surface (HRS) by measuring the ellipsoidal heights (h) of points with known orthometric height (H) or normal height (H*). The ellipsoidal heights are measured directly by means of GPS/GNSS. The height anomaly (ζ=h-H*) or the geoid height (N=h-H) at a given point is directly determined. [8]

3.3.3 Digital finite elements height reference surface (DFHRS)

The finite-element method has been used for modeling the height reference surface (HRS) in the Digital Finite Element Height Reference Surface (DFHRS) project. The DFHRS research project at IAF of the Hochschule Karlsruhe - University of Applied Sciences aims to implement parametric modeling and computation of height reference surfaces for the geometric and the physical observation components in a hybrid adjustment approach (DFHRS). [8]

Access to the parametric HRS model is enabled by DFHRS databases (DFHRS-DB), which allow the direct conversion of GNSS-heights (h) into physical heights (H). DFHRS databases are used for online GNSS-height measurements in DGNSS-networks (SAPOS, AXIONET, etc.) and in the Geographic Information Systems (GIS). The DFHRS-DB has been computed for different states in Germany as well as several nations and regions in Europe, Africa, and the USA. The accuracy of the obtained results varies from 0.01-0.1 meter.

The direct conversion of the ellipsoidal GNSS height h (Ellipsoidal height), determined at the Earth surface, into the physical Earth gravity field-based physical height H, is necessary for GNSS-based height measurements in modern GNSS-positioning services. The basic relation between the GNSS-based height h and the standard height (orthometric height H) in figure (3.4) reads: [8]

$$H = h - N \tag{3-50}$$

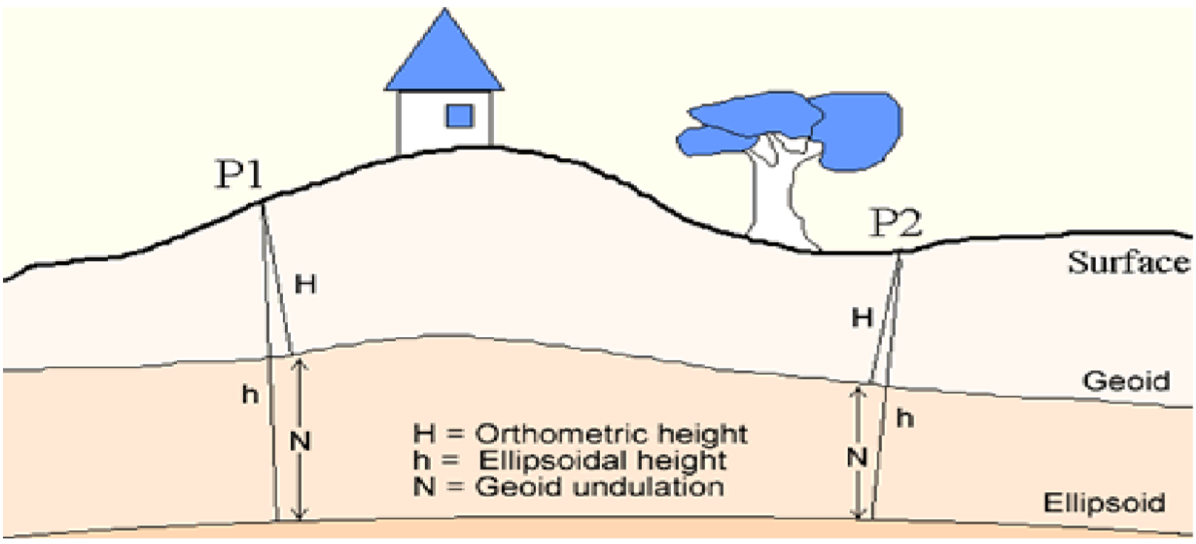

Figure (3.4): The relation between orthometric height H, ellipsoidal heights h and geoid undulation N. [8]

3.3.3.1 Principles of DFHRS

The geoid is represented by its height above the Ellipsoid or the so-called geoid undulation (N). In DFHRS, N is represented by the Finite Element Method (FEM) with polynomial parameters p. These describe a finite element HRS called NFEM (p| λ,ϕ,h). If a scale difference Δm is considered for old reference systems, then the HRS is represented by NFEM (p, Δm | λ,ϕ,h). Equation (3-50) can, therefore, be written as:

$$H = h - DFHRS(p, \Delta m \mid \lambda, \phi, h) \tag{3-51}$$

Or equivalently:

$$H = h - NFEM(p, \Delta m \mid \lambda, \phi, h) \tag{3-52}$$

The finite element representation NFEM(p|x,y) is carried out by bivariate polynomials of degree n, which are set up in regular or irregular meshes. If we describe with p^i the polynomial coefficients ($a_{00}, a_{10}, a_{01}, a_{20}, a_{11}, a_{02}, \ldots$) of the i-th mesh of n meshes in total, the height NFEM(p^i|x,y) of the HRS over the ellipsoid is:

$$\mathrm{NFEM}\left(\mathrm{p^i}\middle|\mathrm{x,y}\right) = \mathrm{f(x,y)^T p^i} \tag{3-53}$$

$$p^i = \left[{p_{jk}}^i\right]^T; j = 0, n; k = 0, n \; and \; f(x,y)^T = (1, x, y, x^2, xy, y^2, \ldots) \tag{3-54}$$

The principle of the DFHRS is to divide an area or region of a continuous HRS into a number of patches, with each patch further divided into a number of meshes as shown in figure (3.5). Each patch has a datum and associated transformation parameters (d) and each mesh has HRS parameters (p). Continuity conditions must also be considered. The NFEM for a point in the boundary between two meshes should be the same depending on the two meshes (the so-called C0- continuity), as should the slope at the boundary for both meshes (so-called C1-continuity) so that the meshes represent the whole area. The DFHRS parameters (p) and the mesh information are stored in the DFHRS-DB. [8]

The DFHRS geometrical observations include points with ellipsoidal (h) and normal or orthometric heights(H) as identical points, geoid heights form global or regional geoid models, astronomical deflections of the vertical (ξ,η) from geoid models and the points with observed ellipsoidal heights(h) or orthometric heights (H). [8]

The parameters stored in the DFHRS-DB are (p, Δm) and are related to the projected coordinates (x,y). The polynomial representation of the DFHRS is written in terms of design matrix ***f*** and parameters vector ***p***:

$$NFEM(p|x,y) = f(x,y)^T p \tag{3-55}$$

The observation equation for an ellipsoidal normal height in the i-th mesh with covariance matrix $\mathrm{C_h}$ has the following observation equation:

$$h + v = H + h\Delta m + f(x,y)^T p^i \quad \text{(3-56a)}$$

The observation equation of a global potential model (GPM) geoid height in the i-th mesh and the j-th patch is:

$$N_{GPM} + v = f(x,y)^T p^i + \partial N(d^j) \quad \text{(3-56b)}$$

The deflections of the vertical in the i-th mesh and j-th patch observation equations are:

$$\xi + v = \frac{-f_\phi^T}{M(\phi)+h} p^i + \partial\xi\left(d^j_{\eta.\xi}\right) \quad \text{(3-56c)}$$

$$\eta + v = \frac{-f_L^T}{N(\phi)\cos(\phi)+h} p^i + \partial\eta\left(d^j_{\eta,\xi}\right) \quad \text{(3-56d)}$$

The observation equation for the physical (orthometric or normal) heights reads:

$$H + v = H \quad \text{(3-56e)}$$

The continuity conditions between different neighbor meshes are considered as additional observation equations:

$$C + v = C(p) \quad \text{(3-56f)}$$

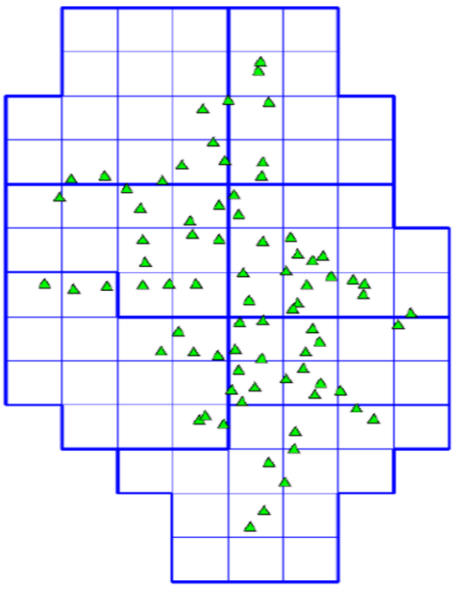

Figure (3.5): DFHRS patches and meshes, where thick lines represent the patch boundary and thin lines represent the meshes. [8]

In the equations (3-56a) to (3-56f), $\partial N(d)$ is the datum parameterization of the GPM quasigeoid or geoid grid heights in the patch. $\partial\xi(d)$ and $\partial\eta(d)$ are datum parameterizations

of the deflections of the vertical. f_{ϕ} is the partial derivative of *f(x,y)* with respect to the latitude. And finally, $f_{\boldsymbol{L}}$ is the partial derivative of *f(x,y)* with respect to longitude. [8]

To reduce the effect of medium- or long-wavelength systematic shape deflections, specifically the natural and stochastic "weak shapes", in the observations N and (ξ,η) from geoid or GPM models, these observations are subdivided into a number of patches; see the thick blue in figure(3.5). [8]

3.3.3.2 Extension of DFHRS to physical observations

The DFHRS physical observations include terrestrial, airborne and spaceborne gravity measurements. In addition, physical observations from a global or regional geopotential model (GPM) of the Earth gravitational potential V for limited size cap area and cap pole, represented by the so-called SCH (*Snm* ', *Cnm* '). [8]

The advantage of SCH is that the number of parameters for the local cap area is significantly less than that needed in an ordinary global SH model.

$$T(r,\alpha,\theta)=\sum_{k=0}^{k\,max}\left(\frac{R}{r}\right)^{n(k)+1}\sum_{m=0}^{k}\left(C'_{n(k),m}\cos m\alpha+S'_{n(k),m}\sin m\alpha\right)\,P_{n(k),,m}(\cos\theta) \tag{3-57}$$

The DFHRS model can be used in SCH as a condition so that NFEM=N(SCH).

$$v_{\Delta N}=N\left(C'_{n(k),m},S'_{n(k),m}\right)-f^{T}p \tag{3-58}$$

The gravity observation $\mathbf{g_p}$ at the Earth's surface, taken with a gravity meter, refers to the local astronomical vertical system (LAV). The respective observed three-dimensional gravity vector in total is given by:

$$\mathrm{g}^{\mathrm{LAV}}=\left[0,0,-\mathrm{g_p}\right]^{\mathrm{T}} \tag{3-59a}$$

The related gravity anomaly is $\Delta g=g_P-\gamma_Q$. The gravity vector can be rotated using the deflections of the vertical (ξ,η) or equivalently by the astronomical latitude and longitude ($\Phi=\phi+\xi,\ \Lambda=\lambda+\eta\ /\ \cos(\phi)$) to the Earth-centered Earth-fixed system (ECEF) using (Φ,Λ), Following this rotation, the centrifugal parts are removed, and the original observation in equation (3-59a) is strictly reduced with respect to deflections of the vertical and the

centrifugal acceleration. After a further rotation to the local geodetic vertical system (LGV) related to the cap sphere, the reduced observation (3-59a) is: [8]

$$\Delta g_{red}^{LGV} = [\Delta g_N, \Delta g_E, \Delta g_r]^T \tag{3-59b}$$

Transformation Equations from LAV to LGV:

$$\Phi = \phi + \xi \tag{3-T1}$$

$$\Lambda = \lambda + \frac{\eta}{\cos(\phi)} \tag{3-T2}$$

$$\vec{g}_{LGV} = \begin{bmatrix} g_\phi \\ g_\lambda \\ g_r \end{bmatrix} = R_{LAV}^{LGV}\ \vec{g}_{LAV} \tag{3-T3}$$

$$\mathbf{R_{LAV}^{LGV}} = \begin{bmatrix} \sin\phi \sin\Phi \cos(\Lambda-\lambda) + \cos\phi\cos\Phi & \sin\phi\sin(\Lambda-\lambda) & \cos\phi\sin\Phi - \sin\phi\cos\Phi\cos(\Lambda-\lambda) \\ -\sin\Phi\sin(\Lambda-\lambda) & \cos(\Lambda-\lambda) & \cos\Phi\sin(\Lambda-\lambda) \\ \sin\phi\cos\Phi - \cos\phi\sin\Phi\cos(\Lambda-\lambda) & -\cos\Phi\sin(\Lambda-\lambda) & \cos\phi\cos\Phi\cos(\Lambda-\lambda) + \sin\phi\sin\Phi \end{bmatrix} \tag{3-T4}$$

$$\vec{g}_e = \begin{bmatrix} g_X \\ g_Y \\ g_Z \end{bmatrix} = R_{LGV}^{e}\,\vec{g}_{LGV} \tag{3-T5}$$

$$R_{LGV}^{e} = \begin{bmatrix} -\sin\phi\cos\lambda & -\sin\lambda & \cos\phi\cos\lambda \\ -\sin\phi\sin\lambda & \cos\lambda & \cos\phi\sin\lambda \\ \cos\phi & 0 & \sin\phi \end{bmatrix} \tag{3-T6}$$

$$\vec{z} = \omega^2\vec{P} = \begin{bmatrix} \omega^2 X \\ \omega^2 Y \\ 0 \end{bmatrix} \tag{3-T7}$$

$$\vec{g}_e{}' = \begin{bmatrix} g'_X \\ g'_Y \\ g'_Z \end{bmatrix} = \begin{bmatrix} g_X \\ g_Y \\ g_Z \end{bmatrix} = \begin{bmatrix} \omega^2 X \\ \omega^2 Y \\ 0 \end{bmatrix} \tag{3-T8}$$

In the SCH frame (3-59b) using the transformation equations (3-T1) to (3-T8) is written as:

$$\Delta g_{grav}^{SCH} = \left[\frac{1}{r}\frac{\partial T}{\partial\theta}, \frac{1}{r\sin\theta}\frac{\partial T}{\partial\alpha}, \frac{\partial T}{\partial r}\right]^T \tag{3-59c}$$

The harmonic expansion of the radial component of equation (3-59c) is:

$$\Delta g_{grav}^{SCH} = \sum_{k=0}^{\infty} \left(\frac{R}{r}\right)^{n(k)+1} \frac{(n(k)+1)}{r} \left(\sum_{m=0}^{k} \left(C'_{n(k),m} \cos m\alpha + S'_{n(k),m} \sin m\alpha\right) P_{n(k),m}(\cos\theta)\right) + dg(d_g) \quad (3\text{-}59d)$$

The SCH has an integer order m and a real degree n_k. The real degree n_k satisfies the property of orthogonality of the function in the cap area. These represent the roots of Legendre function and its derivatives according to the following conditions:

$$P_{nk(m)}(\cos(\theta)) = 0 \qquad \text{for} \quad k\text{-}m = \text{odd} \quad (3\text{-}60a)$$

$$\frac{dP_{nk(m)}(\cos(\theta))}{d\theta} = 0 \qquad \text{for} \quad k\text{-}m = \text{even} \quad (3\text{-}60b)$$

This principle has disadvantages, because of the need to search for the real degrees n_k according to the conditions in equations (3-60a) and (3-60b). The different algorithms for calculating the roots of Legendre functions introduce additional errors because they are mostly iterative with certain approximations or complicated algorithms. Furthermore, the computation of the real degree $n_k$is time-consuming. The calculations of Legendre functions and their derivatives with non-integer degrees, where no recursive formulas are given in the literature, is also a time-consuming process making use of approximations. [8]

3.3.4 Least Squares Collocation

The basic principle of the Least Squares Collocation (LSC) is that the disturbing potential T satisfies Laplace's equation. It is represented a by a group of suitable harmonic base functions φ_k at given positions with their related coefficients. In this case, the disturbing potential reads:

$$T(P) = f(P) = \sum_{k=1}^{q} b_k \varphi_k \quad (3\text{-}61)$$

The measurements are assumed to be linear functionals L(T) of the disturbing potential T. The linear operators of deflections of the vertical, gravity anomalies and gravity disturbances related to the disturbing potential are given in table (3.2). [8]

Table (3.2): The potential related observations and their linear operators L(T) [8]

Variable	**Relation to the potential**	**L(T)**
Deflection of vertical east-west	$-\frac{1}{\gamma_Q(N+h)\cos\phi}\frac{\partial T}{\partial \lambda}$	$-\frac{1}{\gamma_Q(N+h)\cos\phi}\frac{\partial}{\partial \lambda}$
Deflection of vertical north-south	$-\frac{1}{\gamma_Q(M+h)}\frac{\partial T}{\partial \phi}$	$-\frac{1}{\gamma_Q(M+h)}\frac{\partial}{\partial \phi}$
Gravity anomalies	$-\frac{\partial T}{\partial z}-\frac{2}{R}T$	$-\frac{\partial}{\partial Z}-\frac{2}{R}$
Gravity disturbance	$-\frac{\partial T}{\partial z}$	$-\frac{\partial}{\partial z}$

For a given observation I, we have:

$$\sum_{i=1}^{q} B_{ik} b_K = l_i \tag{3-62}$$

For a given observation I, we have:

$$B_{ik} = L_i(\varphi_k) \tag{3-63}$$

In equation (3-62), we can solve for q coefficients by using q observations. This method is called collocation. If we consider a harmonic covariance propagation function (K) that is symmetric with respect the point P and the reference point Q, the base function φ_k related to the observation type of Q is:

$$\varphi_K = L_K^Q K(P,Q) = C_{PK} \tag{3-64}$$

Substituting (3-64) in (3-63) results in:

$$B_{ik} = L_i^P L_K^Q K(P,Q) = C_{ik} \tag{3-65}$$

Solving (3-62) for and substituting in (3-61) results in:

$$f(P) = [C_{P1} \quad C_{P2} \quad \cdots \quad C_{Pq}] \begin{bmatrix} C_{11} & C_{12} & \cdots & C_{1q} \\ C_{21} & C_{22} & \cdots & \vdots \\ \vdots & \vdots & \ddots & \vdots \\ C_{q1} & C_{q2} & \cdots & C_{qq} \end{bmatrix}^{-1} \begin{bmatrix} l_1 \\ l_2 \\ \vdots \\ l_q \end{bmatrix} \tag{3-66}$$

The covariance propagation function K as given by reads:

$$K(P,Q) = \sum_{n=2}^{\infty} \sigma_n^2 \left(\frac{R^2}{r_P r_Q}\right)^{n+!} P_n(\psi_{PQ}) \quad (3\text{-}67)$$

In equation (3-67), σ_n^2 is the n-th degree variance that can be theoretically calculated by the Tscherning & Rapp method or from the global gravity models. ψ_{PQ} is the spherical distance between the points P and Q.

The greatest advantage of LSC is the flexibility in estimating any kind of the potential related quantities using a combination of all available geodetic physical and geometrical observations, in addition to its proper use for local and global implementation. The primary problem, however, is that for huge areas a large amount of data would be required. This requires extended computation time of the new points. [8]

3.4 Integrated Geodesy

High-speed computers allowed the processing of large amounts of data of different types to solve a large system of equations. The integrated data processing for a unified model for three-dimensional geodesy is called “Integrated Geodesy”. In the classical geodesy, only one type of observation is used for gravity field modeling. An example of the classical geodesy is the Stokes formula for geoid modeling, where only the gravity anomalies are used to compute the disturbing potential T. [8]

The principle of Integrated Geodesy is that any time independent observation l can be expressed as a function with parameters vector $\boldsymbol{p}$ depending on the position (Geometry) $\vec{x} = (X, Y, Z)$ and the Earth's potential W.

$$l = l\big(\vec{x}, W(\vec{x}, p)\big) \quad (3\text{-}68)$$

In most cases, the position (geometry) is assumed to be fixed. The parameterization is to model the potential and its related quantities. The quantities introduced in a chapter (3.2.5) are all functions of the potential that apply to equation (3-68). The DFHRS described in a chapter (3.3.2) also qualifies as Integrated Geodesy. [8]

3.5 State of the art in the gravity field modeling

There currently exist many published global, regional and local geoids. In the global models, they are mostly modeled by means of SH as described in the chapter (3.2).

EGM2008 is the global combined gravity model with the highest degree and order presently available, with a maximum degree and order of 2190. The EGM2008 would satisfy a 5cm geoid height accuracy, in case it would be free of "weak shapes". Other combined global gravity models were calculated and introduced by GFZ-Potsdam (EIGEN models). The most recent of these is the EIGEN06c, which has a maximum degree and order of 1420. In the geoid heights, the accuracy of the EIGEN06c is comparable to the EGM2008. Other combined models with less degree and order (EIGEN01-05c) are up to degree and order of 360. [8]

The estimation of high degree and order models like EGM2008 and EIGEN06c have introduced new calculation methods. In these methods, the parameters are calculated using a combination of integrals and least squares. Figure (3.6) shows the use of different data types, and how they contribute to finding the harmonic coefficients of the EIGEN06c model.

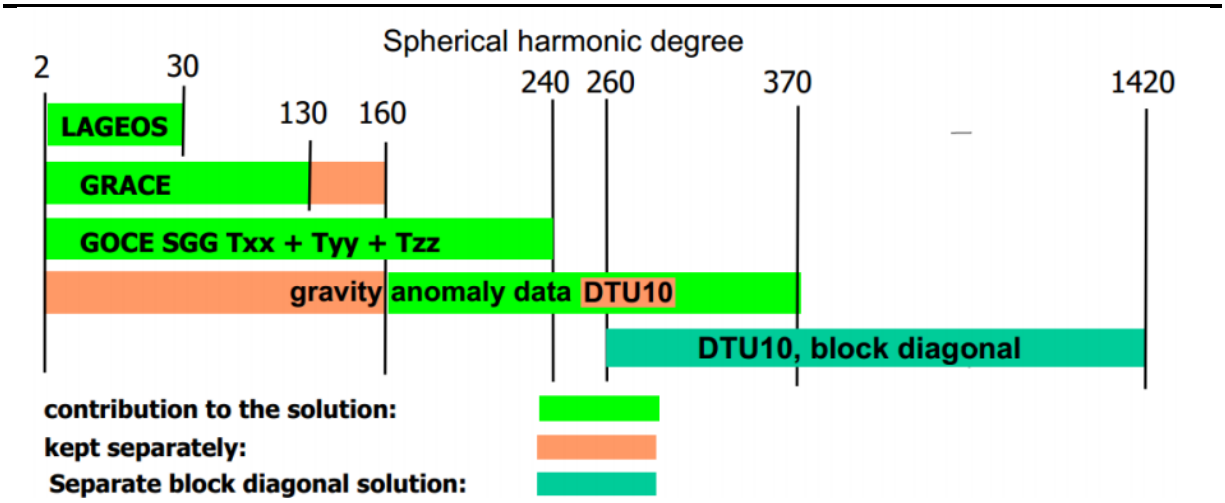

Figure (3.6): The principle of harmonic coefficients calculation in the EIGEN06c model. [8]

For modeling the satellite-only gravity data, which are free of datum and zero level, satellite-only models are always introduced. One of the most common applications is the satellite orbit determination. These models, however, suffer from problems associated with ground geoid determination. This is because of low degrees and orders due to the loss of data, especially in pole areas. Table (3.3) shows selected combined and satellite-only models and their related maximum degree and order with the accuracy of the model. [8]

Table (3.3): Examples of satellite-only and combined global geoid models. [8]

Model	Publishing date	N-max	Data	Geoid accuracy in Europe (m)
EGM2008	2008	2190	S(GRACE),G,A	0.208 m
EIGEN06c	2011	1420	S(GOCE,GRACE,LAGEOS),G ,A	0.214 m
EIGEN06s	2011	240	S(GOCE,GRACE,LAGEOS)	0.449 m
GGM03c	2009	360	S(GRACE),G,A	0.515 m
GGM03s	2008	150	S(GRACE)	1.416 m

Data: S=Satellite data, G = Terrestrial gravity, A = height fitting points

The EGG07, computed by IfE-Hannover, is one of the latest regional gravity models in Europe and has supplanted the European quasigeoid EGG97. The EGG07 was calculated by the remove-restore method with updated terrestrial gravity, marine gravity, and airborne gravity data. When compared to GPS/leveling heights the EGG07 has an RMSE of 0.01- 0.06 m. The worst results were in high mountains in Austria and France. Another regional geoid model was calculated by the DFHRS software for the Baltic countries (Latvia, Estonia, and Lithuania). The achieved accuracy of the Baltic geoid was 1-3cm. For Europe, a geoid model using DFHRS software was calculated in 2004 with an accuracy of better than 10 cm. [8]

In terms of local geoid models, the USGG09 and GEOID09 were introduced in 2010 for the United States of America by the NGS (National Geodetic Survey). The USGG09 is an absolute gravimetric geoid model using the remove-restore method using millions of land and ocean gravity data points with EGM96 support for longwave geoid heights. The combined geoid model (GEOID09) is applied by combining the USGG09 with nearly 20000 GPS/leveling points using Multi-Matrix Least Squares collocation (MMLSC). In the GEOID09 six LSC matrices were applied to achieve 2km geoid resolution with RMSE of 1.5cm. [8]

In Germany, the German Combined Quasi geoid 2011(GCG2011) was introduced by the Bundesamt für Kartographie und Geodäsie (BKG) and IfE-Hannover. The GCG2011 was calculated by the remove-restore method combined with point mass method using terrestrial gravity, GOCE gravity, and GPS/leveling points. The GCG2011 accuracy is 1-2 cm in flat and hilly areas but is reduced to approximately 3-4 cm in the high mountains. In ocean areas, the accuracy of the GCG2011 geoid is in the range of 4-10cm. [8]

In 2010, the DFHRS software was used to calculate the Height Reference Surface (Quasigeoid) for the State of Moldova. The solution was applied using a mesh design of 5x5km. In Moldova, there are two height systems in use. One system is for urban areas, while the other is for rural areas. For this reason, the solution was done twice by preparing two DFHRS-DBs. Field tests have shown an average accuracy of 1-2 cm over the entire country. [8]

Chapter Four:

Data and Analysis

4.1 Introduction.

4.2 Global Evaluation of the Geoid Models.

4.3 Local Evaluation of the Geoid Models.

Data and Analysis

4.1 Introduction

The International Centre for Global Earth Models (ICGEM) is one of five services coordinated by the International Gravity Field Service (IGFS) of the International Association of Geodesy (IAG). The primary task of the ICGEM is making all global gravity field models of the Earth available to the public. The models can be downloaded on the ICGEM website in a standardized self-explanatory format as spherical harmonic coefficients. ICGEM provides not only the most recent, but also historical models, and provides a Digital Object Identifier (DOI) services for gravitational models since 2015. Gravity field differences, their time variation, and different gravity field model functionals are available via a dedicated gravity function calculation service and visualization tool provided on the ICGEM website. In addition, the web site offers tutorials on spherical harmonics and the underlying theory of the calculation service. [9]

The ICGEM service which was established in 2003 as a new service of International Gravity Field Service (IGFS) continues to make the global gravity field models available to the public. The service does not only provide the model coefficients publicly available but also presents an interactive platform for the interested users to calculate and visualize the global gravity field functionals and also a discussion forum for users to raise their questions or convey their messages and feedback. Since the beginning of the service, the user profile has changed and widely expanded. Now, users practicing other disciplines (e.g., planetary science, geology) or users working in the industry, mapping companies, and agencies are also interested in ICGEM products and they communicate the ICGEM team closely for further information and analyses. [9]

In order for users to benefit the current ICGEM products and coming GRACE-FO mission products more efficiently, ICGEM has launched the new ICGEM service which is designed to improve the users' experience with the service outcomes. Also, the new service is more flexible from the point of administration and promises continuous improvement. The new ICGEM website is designed to encourage the researchers to use the latest model products for education and research purposes. [9]

The Calculation Service

An improved user-friendly web-interface to calculate gravity functionals from the spherical harmonic models on freely selectable grids, with respect to a reference system of the user's choice, is provided. The following functionals are available for gravity field model computations:

- pseudo height anomaly on the ellipsoid (or at arbitrary height over the ellipsoid).
- height anomaly (on the Earth's surface as defined).
- geoid height (height anomaly plus spherical shell approximation of the topography).
- gravity disturbance.
- gravity disturbance in spherical approximation (at arbitrary height over the ellipsoid).
- gravity anomaly (classical and modern definition).
- gravity anomaly (in spherical approximation, at arbitrary height over the ellipsoid).
- simple Bouguer gravity anomaly.
- gravity on the Earth's surface (including the centrifugal acceleration).
- gravity on the ellipsoid (or at arbitrary height over the ellipsoid, including the centrifugal acceleration).
- gravitation on the ellipsoid (or at arbitrary height over the ellipsoid, without centrifugal acceleration)
- potential on the ellipsoid (or at arbitrary height over the ellipsoid, without centrifugal potential).
- second derivative in a spherical radius direction of the potential (at arbitrary height over the ellipsoid).
- equivalent water height (water column).

Filtering is possible by selecting the maximum degree of the used coefficients or the filter length of a Gaussian averaging filter. The models from dedicated time periods (e.g. coefficients of monthly solutions from GRACE) are also available after non-isotropic smoothing (decorrelation). [10]

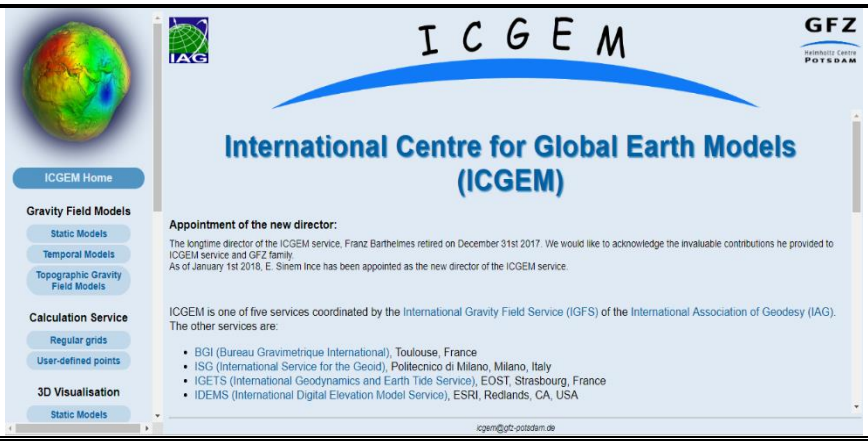

Figure (4.1): ICGEM Site. [11]

Root-Mean-Square Error (RMSE)

The root-mean-square error (RMSE) (or sometimes root-mean-squared error) is a frequently used measure of the differences between values (sample or population values) predicted by a model or an estimator and the values observed. The RMSE represents the square root of the second sample moment of the differences between predicted values and observed values or the quadratic mean of these differences. These deviations are called residuals when the calculations are performed over the data sample that was used for estimation and are called errors (or prediction errors) when computed out-of-sample. The RMSE serves to aggregate the magnitudes of the errors in predictions for various times into a single measure of predictive power. RMSE is a measure of accuracy, to compare forecasting errors of different models for a particular dataset and not between datasets, as it is scale-dependent.

RMSE is always non-negative, and a value of 0 (almost never achieved in practice) would indicate a perfect fit to the data. In general, a lower RMSE is better than a higher one. However, comparisons across different types of data would be invalid because the measure is dependent on the scale of the numbers used.

RMSE is the square root of the average of squared errors. The effect of each error on RMSE is proportional to the size of the squared error; thus, larger errors have a disproportionately large effect on RMSE. Consequently, RMSE is sensitive to outliers.

4.2 Global Evaluation of the Geoid Models.

The following table (4.1) shows a comparison of quasigeoid heights derived from the models with GPS / leveling derived geoid values from the USA, Europe, and Global.

Table (4.1): Global Evaluation of the Geoid Models.

Model	Year	N max	Europe (1047 Points)	USA (6169 Points)	Global (12036 Points)
EGM96	1996	360	0.493	0.379	0.4267
EGM2008	2008	2190	0.125	0.248	0.2397
EIGEN-5C	2008	360	0.266	0.341	0.3422
EIGEN6C4	2014	2190	0.121	0.247	0.2361
XGM2019e-2159	2019	2190	0.127	0.248	0.2361

4.3 Local Evaluation of the Geoid Models.

4.3.1 Local Evaluation Steps

To evaluate the accuracy of the different geoid models, a group of precise leveling benchmarks was measured by classical GNSS methods (RTK). The ellipsoidal height (h) by GNSS and the orthometric height (H) by precise leveling provide a local geoid separation at the point (N). Geoid separation was calculated from the original global models and local models typically uploaded to the GNSS receivers. The differences were statistically analyzed to provide general descriptions. Also, local geoid fitting approaches were tested to enhance the accuracy of the global models, table (4.2) shows the ellipsoidal height (h), orthometric height (H) and Geoid height (N) of the group of precise leveling benchmarks that were measured, and the figure (4.2) shows the distribution of precise leveling benchmarks that were measured in Palestine.

Table (4.2): Ellipsoidal height (h), Orthometric height (H) and Geoid height (N) of the group of precise leveling benchmarks in Palestine.

Point Number	H	h	h-H (N)
1	894.017	912.945	18.928
2	752.222	771.443	19.221
3	946.798	966.502	19.704
4	-277.637	-259.815	17.822
5	-18.151	-0.253	17.898
6	-225.014	-206.304	18.71
7	-242.845	-223.522	19.323
8	-273.399	-253.984	19.415
9	-250.618	-230.884	19.734

Figure (4.2): The distribution of the group of precise leveling benchmarks in Palestine.

4.3.2 EGM96 Evaluation

EGM96 (Earth Gravitational Model 1996) is a geopotential model of the Earth consisting of spherical harmonic coefficients complete to degree and order 360.

EGM96 is a composite solution, consisting of, a combination solution to degree and order 70, a block diagonal solution from degree 71 to 359, and the quadrature solution at degree 360, figure (4.3) show the Palestine Geoid Model (EGM96). [12].

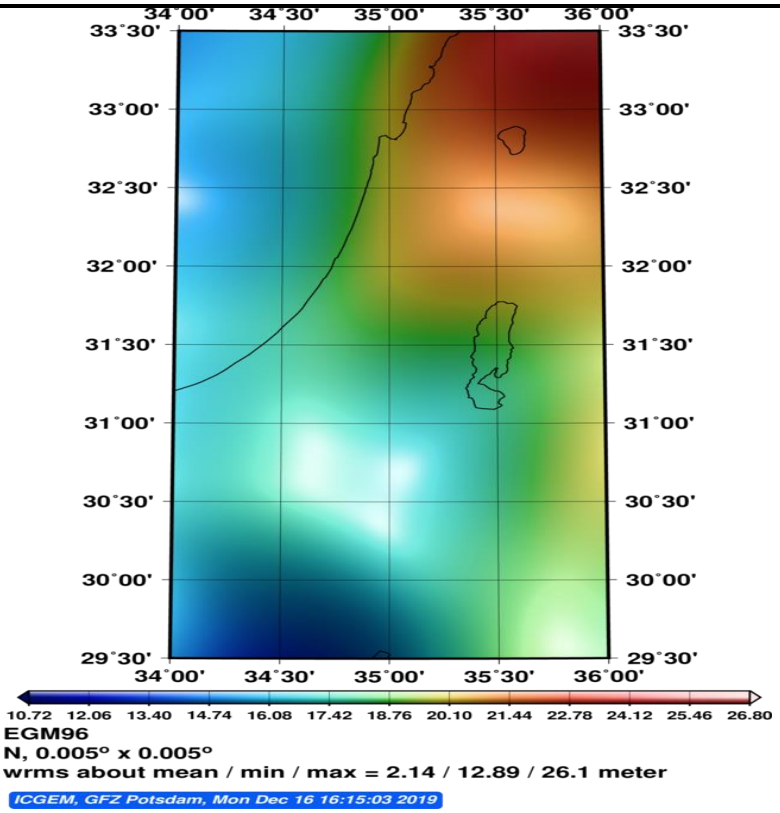

Figure (4.3): Palestine Geoid Model (EGM96). [11]

The results obtained from the EGM96 geoid model system can be summarized in table (4.3).

Table (4.3): Result of the Geoid Height from (EGM96).

Point Number	h-H (N Field	N (EGM96)	ΔN
1	18.928	18.626	-0.302
2	19.221	18.389	-0.832
3	19.704	19.010	-0.694
4	17.822	19.942	2.120
5	17.898	18.982	1.084
6	18.710	19.985	1.275
7	19.323	20.610	1.287
8	19.415	20.667	1.252
9	19.734	20.973	1.239

Minimum Value	-0.832
Maximum Value	2.120
RMSE	1.290

In the (EGM96) Geoid model, after inserting points to the ICGEM site and obtaining the results, it was found that the minimum value is equal to -0,832, and maximum value is equal to 2.120, this means that the height difference between Geoid height from EGM96 Geoid model and Geoid height from the field (GNSS and precise leveling) Does not give a fixed number, but ranging from the minimum value to the maximum value and this rang is large, also it was found that the root mean square error value is equal to 1.290 this value is relatively large, this means that the differences between Geoid height from EGM96 Geoid model and Geoid height from the field (GNSS and precise leveling) are large.

4.3.3 EGM2008 Evaluation

EGM2008 is a spherical harmonic model of the Earth's gravitational potential, developed by a least-squares combination of the ITG-GRACE03S gravitational model and its associated error covariance matrix, with the gravitational information obtained from a global set of area-mean free-air gravity anomalies defined on a 5 arc-minute equiangular grid. This grid was formed by merging terrestrial, altimetry-derived, and airborne gravity data. Over areas where only lower resolution gravity data were available, their spectral content was supplemented with gravitational information implied by the topography. EGM2008 is complete to degree and order 2159 and contains additional coefficients up to degree 2190 and order 2159. Over areas covered with high-quality gravity data, the discrepancies between

EGM2008 geoid undulations and independent GPS/Leveling values are on the order of ±5 to ±10 cm, figure (4.4) shows the Palestine Geoid Model (EGM2008). [13]

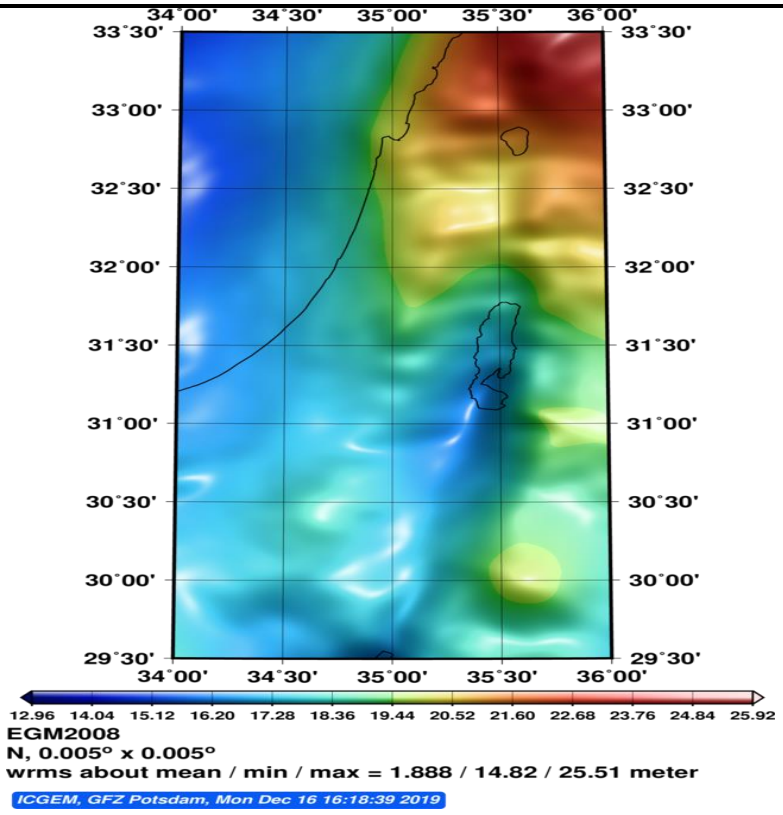

Figure (4.4): Palestine Geoid Model (EGM2008). [11]

The results obtained from the EGM2008 geoid model system can be summarized in table (4.4).

Table (4.4): Result of the Geoid Height from (EGM2008).

Point Number	h-H (N Field)	N (EGM2008)	ΔN
1	18.928	18.740	-0.188
2	19.221	18.568	-0.653
3	19.704	19.035	-0.669
4	17.822	17.662	-0.160
5	17.898	17.692	-0.206
6	18.710	18.605	-0.105
7	19.323	19.236	-0.087
8	19.415	19.318	-0.097
9	19.734	19.938	0.204

Minimum Value	-0.669
Maximum Value	0.204
RMSE	0.362

In the (EGM2008) Geoid model, after inserting points to the ICGEM site and obtaining the results, it was found that the minimum value is equal to -0.669, and maximum value is equal to 0.204, this means that the height difference between Geoid height from EGM2008 Geoid model and Geoid height from the field (GNSS and precise leveling) Does not give a fixed number, but ranging from the minimum value to the maximum value and this rang is small, also it was found that the root mean square error value is equal to 0.362 this value is relatively small, this means that the differences between Geoid height from EGM2008 Geoid model and Geoid height from the field (GNSS and precise leveling) are small.

4.3.4 EIGIN-5C Evaluation

The combined gravity field model EIGEN-5C is an upgrade of EIGEN-GL04C. The model is a combination of GRACE and LAGEOS mission data plus 0.5 x 0.5 degrees gravimetry and altimetry surface data. The combination of the satellite and surface data has been done by the combination of normal equations, which are obtained from observation equations for the spherical harmonic coefficients, figure (4.5) shows the Palestine Geoid Model (EIGIN-5C) [14]

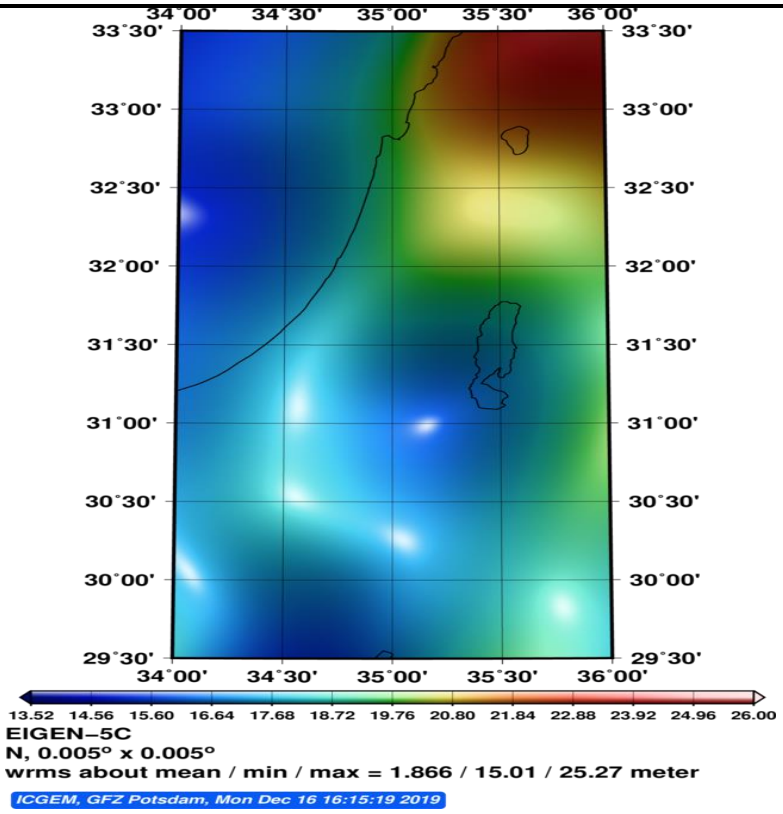

Figure (4.5): Palestine Geoid Model (EIGIN-5C). [11]

The results obtained from the EIGEN-5C geoid model system can be summarized in table (4.5).

Table (4.5): Result of the Geoid Height from (EIGEN-5C).

Point Number	h-H (N Field)	N (EIGEN-5C)	ΔN
1	18.928	17.748	-1.180
2	19.221	17.567	-1.654
3	19.704	18.049	-1.655
4	17.822	18.075	0.253
5	17.898	18.036	0.138
6	18.710	19.246	0.536
7	19.323	19.975	0.652
8	19.415	20.041	0.626
9	19.734	20.388	0.654

Minimum Value	-1.655
Maximum Value	0.654
RMSE	1.030

In the (EIGEN-5C) Geoid model, after inserting points to the ICGEM site and obtaining the results, it was found that the minimum value is equal to -1.655, and maximum value is equal to 0.654, this means that the height difference between Geoid height from EIGEN-5C Geoid model and Geoid height from the field (GNSS and precise leveling) Does not give a fixed number, but ranging from the minimum value to the maximum value and this rang is large, also it was found that the root mean square error value is equal to 1.030 this value is relatively large, this means that the differences between Geoid height from EIGEN-5C Geoid model and Geoid height from the field (GNSS and precise leveling) are large.

4.3.5 EIGIN-6C4 Evaluation

EIGEN-6C4 is a static global combined gravity field model up to degree and order 2190. It has been elaborated jointly by GFZ Potsdam and GRGS Toulouse. The combination of the different satellite and surface data sets has been done by a band-limited combination of normal equations (to max degree 370), which are generated from observation equations for the spherical harmonic coefficients. A brief description of the applied techniques for the generation of such a combined gravity field model is given in Shako et al. 2014. The resulted solution to degree/order 370 has been extended to degree/order 2190 by a block diagonal solution using the DTU10 global gravity anomaly data grid. [15]

EIGEN-6C4 is a high-resolution global gravity field model. It is one of the first EIGEN (European Improved Gravity model of the Earth by New techniques) combination model that

includes GOCE data. Its role is fundamental in geodesy and Earth sciences and ranges from practical purposes, like orbit determination, to scientific applications, like the investigation of the density structure of the Earth's interior. The new EIGEN released in 2014 is called EIGEN-6C4 and has been created from a combination of a multitude of data, figure (4.6) shows the Palestine Geoid Model (EIGIN-6C4) [15]

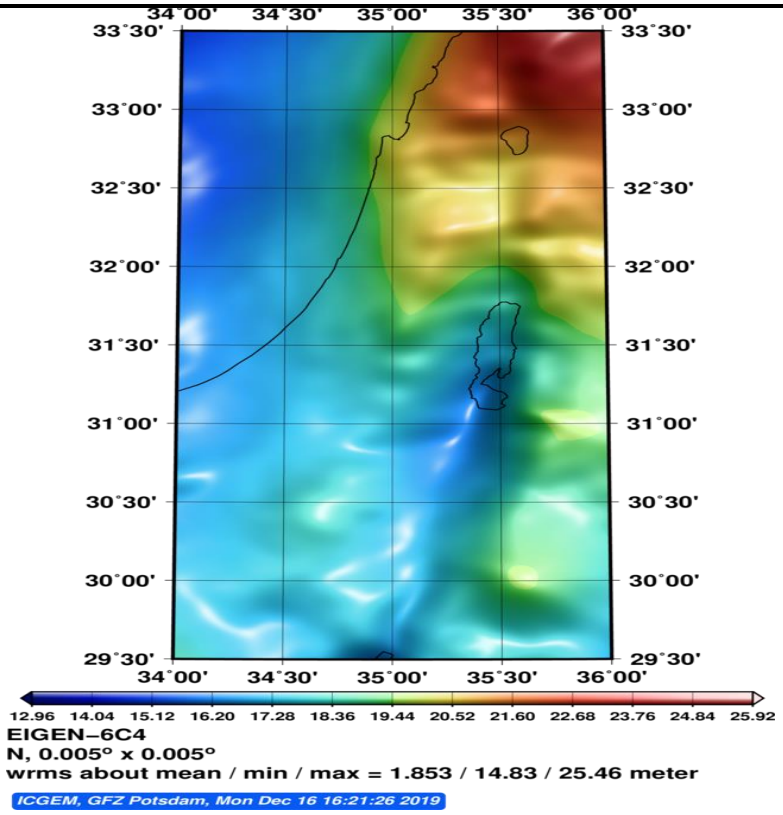

Figure (4.6): Palestine Geoid Model (EIGEN-6C4). [11]

The results obtained from the EIGEN-6C4 geoid model system can be summarized in table (4.6).

Table (4.6): Result of the Geoid Height from (EIGEN-6C4).

Point Number	h-H (N Field)	N (EIGEN-6C4)	ΔN
1	18.928	18.801	-0.127
2	19.221	18.629	-0.592
3	19.704	19.103	-0.601
4	17.822	17.699	-0.123
5	17.898	17.729	-0.169
6	18.710	18.658	-0.052
7	19.323	19.287	-0.036
8	19.415	19.370	-0.045
9	19.734	19.975	0.241

Minimum Value	-0.601
Maximum Value	0.241
RMSE	0.323

In the (EIGEN-6C4) Geoid model, after inserting points to the ICGEM site and obtaining the results, it was found that the minimum value is equal to -0.601, and maximum value is equal to 0.241, this means that the height difference between Geoid height from EIGEN-6C4 Geoid model and Geoid height from the field (GNSS and precise leveling) Does not give a fixed number, but ranging from the minimum value to the maximum value and this rang is small, also it was found that the root mean square error value is equal to 0.323 this value is relatively small, this means that the differences between Geoid height from EIGEN-6C4 Geoid model and Geoid height from the field (GNSS and precise leveling) are small.

4.3.6 XGM2019_2159 Evaluation

XGM2019e combined global gravity field model from the Technical University of Munich is available in three different expansions. The coefficients are precalculated in the spheroidal harmonic domain and then converted into spherical harmonics and available as "XGM2019e" up to spherical harmonic d/o 5540, "XGM2019e_2159" to 2190, and "XGM2019" up to d/o 760. For different practical reasons, the user can refer to any of the three files. The calculation service results are based on XGM2019e_2159, figure (4.7) shows the Palestine Geoid Model (EIGIN-6C4). [10]

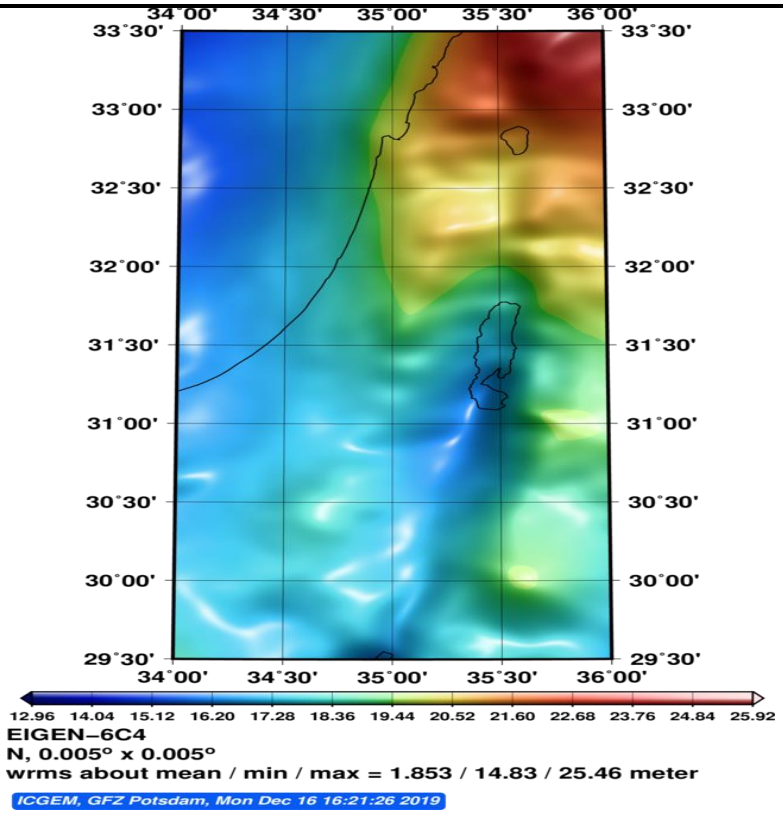

Figure (4.7): Palestine Geoid Model (XGM2019e_2159). [11]

The results obtained from the XGM2019e_2159 geoid model system can be summarized in table (4.7).

Table (4.7): Result of the Geoid Height from (XGM2019e_2159).

Point Number	h-H (N Field)	N (XGM2019e_2159)	ΔN
1	18.928	18.972	0.044
2	19.221	18.718	-0.503
3	19.704	19.197	-0.507
4	17.822	17.875	0.053
5	17.898	17.923	0.025
6	18.710	18.678	-0.032
7	19.323	19.264	-0.059
8	19.415	19.372	-0.043
9	19.734	19.894	0.160

Minimum Value	-0.507
Maximum Value	0.160
RMSE	0.262

In the (XGM2019e_2159) Geoid model, after inserting points to the ICGEM site and obtaining the results, it was found that the minimum value is equal to -0.507, and maximum

value is equal to 0.160, this means that the height difference between Geoid height from XGM2019e_2159 Geoid model and Geoid height from the field (GNSS and precise leveling) Does not give a fixed number, but ranging from the minimum value to the maximum value and this rang is small, also it was found that the root mean square error value is equal to 0.262 this value is relatively small, this means that the differences between Geoid height from XGM2019e_2159 Geoid model and Geoid height from the field (GNSS and precise leveling) are small.

Chapter Five:

Conclusions and Recommendations

5.1 Conclusions.

5.2 Recommendations.

Conclusions and Recommendations

5.1 Conclusions

The accuracy of the different geoid models was evaluated by measure a group of precise leveling benchmarks by the classical GNSS method (RTK). The ellipsoidal height (h) by GNSS and the orthometric height (H) by precise leveling provide a local geoid separation at the point (N). Geoid separation was calculated from the original global models and local models typically uploaded to the GNSS receivers. The differences were statistically analyzed to provide general descriptions. Also, local geoid fitting approaches were tested to enhance the accuracy of the global models.

The final accuracy of the models is represented by the RMSE, the maximum value, and the minimum value in the table (5.1)

Table (5.1): The accuracy of the models.

Model	RMSE	Maximum Value	Minimum Value
EGM96	1.290	2.120	-0.832
EGM2008	0.362	0.204	-0.669
EIGEN-5C	1.030	0.654	-1.655
EIGEN-6C4	0.323	0.241	-0.601
XGM2019e_2159	0.262	0.160	-0.507

It is clear that the best result of accuracy came from (XGM2019e_2159) model, then (EIGEN-6C4) model, then (EGM2008) model and the worse result of accuracy came from (EGM96) model, then (EIGEN-5C) model.

In the (XGM2019e_2159) Geoid model, that the minimum value is equal to -0.507, and maximum value is equal to 0.160, this means that the height difference between Geoid height from XGM2019e_2159 Geoid model and Geoid height from the field (GNSS and precise leveling) Does not give a fixed number, but ranging from the minimum value to the maximum value and this rang is small, also it was found that the root mean square error value is equal to 0.262 this value is relatively small, this means that the differences between Geoid height from XGM2019e_2159 Geoid model and Geoid height from the field (GNSS and precise leveling) are small, so the XGM2019e_2159 Geoid model gives the best result of the accuracy.

In the (EGM96) Geoid model, the minimum value is equal to -0,832, and maximum value is equal to 2.120, this means that the height difference between Geoid height from EGM96 Geoid model and Geoid height from the field (GNSS and precise leveling) Does not give a fixed number, but ranging from the minimum value to the maximum value and this rang is large, also it was found that the root mean square error value is equal to 1.290 this value is relatively large, this means that the differences between Geoid height from EGM96 Geoid model and Geoid height from the field (GNSS and precise leveling) are large, so the EGM96 Geoid model gives the worse result of the accuracy.

5.2 Recommendations

Using the project results, introduce the following recommendation:

- One Geoid Model should be selected as a reference surface to be used directly or after some modification to fit the local Benchmarks in Palestine.
- The necessity of checking the heights obtained from GNSS.
- The triangulation points should be studied according to their height accuracy and measurement methods (barometric leveling, triangulator leveling or precise leveling), recommended to find the location of the Benchmarks in Palestine, if not available, new Benchmarks should be located.

References:

[1] W. Torge, Geodesy 2nd Edition, New Yourk: Walter de Gruyter, 1991.

[2] Dr.Ghadi-Zakarneh, Global navigation satellite System (GNSS), Palestine - Hebron, 2017-2018.

[3] M. Torge and J. Wolfgang, Geodesy 4th Edition, Germany: DE GRUYTER, 2011.

[4] Dr.Ghadi-Zakarneh, Geodesy, Palestine - Hebron, 2017-2018.

[5] L. Q. Q. Zhiping, Geodesy (Introduction to Geodetic Datum and Geodetic System), New Yourk: Springer, 2014 .

[6] P. P. Ph.D Charle, Adjustment Computations 4th Edition, USA: Wiley, 2006.

[7] J. A.Dutton, The Nuture of Geographic Information, USA: Pennstate, 2009.

[8] G. Younis, "Regional Gravity Field Modeling with Adjusted Spherical Cap Harmonics in an Integrated Approach," *Technische Universitat Darmstadt*, no. D17, p. 39, 2013.

[9] "Models and their Evaluations," 2015-2017. [Online]. Available: http://icgem.gfz-potsdam.de/ICGEM-Report_2015-2017. [Accessed 12 4 2019].

[10] "Global gravitational models," 2015. [Online]. Available: http://dataservices.gfz-potsdam.de/mesi/overview.php?id=8. [Accessed 12 5 2019].

[11] "International Centre for Global Earth Models (ICGEM)," 2017. [Online]. Available: http://icgem.gfz-potsdam.de/home. [Accessed 2 5 2019].

[12] "EGM96," 2016. [Online]. Available: https://en.wikipedia.org/wiki/EGM96. [Accessed 2 5 2019].

[13] "The development and evaluation of the Earth Gravitational Model 2008 (EGM2008)," 2012. [Online]. Available: https://agupubs.onlinelibrary.wiley.com/doi/10.1029/2011JB008916. [Accessed 2 5 2019].

[14] "Combined Gravity Field Model EIGEN-5C," 2007. [Online]. Available: http://op.gfz-potsdam.de/grace/results/grav/g007_eigen-05c.html. [Accessed 2 5 2019].

[15] "Integrated Climate Data Center - ICDC," 2014. [Online]. Available: https://icdc.cen.uni-hamburg.de/1/daten/land/geoid-eigen.html. [Accessed 2 5 2019].

[16] "ICGEM," 2014. [Online]. Available: http://dataservices.gfz-potsdam.de/icgem/showshort.php?id=escidoc:1119897. [Accessed 12 5 2019].

List of Acronyms

DFHRF	Digital Finite Elements Height Reference Surface
DFHRS-DB	DFHRS DataBase
DGNSS	Differential GNSS
DTM	Digital Terrain Models
ECEF	Earth-Centered Earth-Fixed system
EGM	Earth Gravitational Model
EIGEN	European Improved Gravity model of the Earth by New techniques
FEM	Finite Element Method
FFT	Fast Fourier Transform
GIS	Geographic Information Systems
GPM	Geopotential Model
GNSS	Global Navigation Satellite Systems
GPS	Global Positioning System
HRS	Height Reference Surface
ICGEM	International Center for Global Gravity Models
IGS	International GNSS Service
IGSN71	International Gravity Standardization Net 1971
ITRF	International Terrestrial Reference Frame
LAV	Local Astronomical Vertical
LGV	Local Geodetic Vertical
LSC	Least Squares Collection
MSL	Mean Sea Level
NGS	National Geodetic Survey
PPP	Precise Point Positioning
RTK	Real Time Kinematic
SH	Spherical Harmonics.
SLR	Satellite Laser Ranging
VRS	Virtual Reference Station
WGS84	World Geodetic System 1984

List of Symbols

a, b	Semi-major and Semi-minor axis of the ellipsoid
m	Mass (kg)
G	Newton's gravitational constant = $6.6742 \times 10^{-11}(m^3 kg^{-2} s^{-2})$
l	Distance
$\vec{F}$	Attraction force
V	Gravitational potential
GM	Gravitational constant of the Earth (Ellipsoid)= $3.986005 \times 10^{14}(m^3 s^{-2})$
ϕ, λ	Geographic latitude and longitude
$\overline{\phi}, \lambda$	Spherical latitude and longitude
$\vec{g}$	Gravity vector
P_{nm}	Legendre function of integer degree and integer order
$P_{nk(m)}$	Legendre function of real degree and integer order
$\overline{S}_{nm}, \overline{C}_{nm}$	Normalized spherical harmonic coefficient
dP_{nm}	Derivative of the Legendre function of integer degree and integer order
$dP_{nk(m)}$	Derivative of the Legendre function of real degree and integer order
W	Gravity potential
H	Orthometric height
h	Ellipsoidal height
x, y	Local/projected coordinates
X,Y, Z	Geocentric cartesian coordinates
Φ, Λ	Astronomical latitude and longitude
Ω	Centrifugal potential of the Earth
ζ	Quasigeoid height (height Anomaly)
γ	Normal gravity of the ellipsoid
ξ	Deflection of vertical in the east-west direction
η	Deflection of vertical in a north-south direction
ω	The angular velocity of the Earth around its major axis
ψ	The Legendre parameter